EPIDERMAL GROWTH FACTOR-MODIFIED PDMS FOR ARTIFICIAL CORNEAS

EPIDERMAL GROWTH FACTOR-MODIFIED POLYDIMETHYLSILOXANE FOR ARTIFICIAL CORNEA APPLICATIONS

By

BETTINA KLENKLER, B.SC.

A Thesis

Submitted to the School of Graduate Studies

in Partial Fulfillment of the Requirements

for the Degree

Doctor of Philosophy

McMaster University

DOCTOR OF PHILOSOPHY (2007) McMaster University

(Chemical Engineering) Hamilton, Ontario

TITLE: Epidermal Growth Factor-Modified Polydimethylsiloxane for Artificial Cornea Applications

AUTHOR: Bettina Klenkler, B.Sc.

SUPERVISOR: Professor Heather Sheardown

NUMBER OF PAGES: xii, 229

Abstract

Improved corneal epithelial cell growth over artificial cornea materials is required to improve device retention within the eye. In this work, varying concentrations of epidermal growth factor (EGF), a potent mitogen for epithelial cells, were immobilized to polydimethylsiloxane (PDMS) substrates, and the cellular response was analyzed.

Three methods were developed to bind EGF to PDMS via polyethylene glycol (PEG) tethers. 1) Plasma Modification: EGF was first reacted with homobifunctional NHS_2PEG and then bound to allylamine plasma-modified PDMS. 2) Hydrosilylation: PDMS was modified with heterobifunctional allyl-PEG-NHS and then EGF was attached to the surface-bound PEG. 3) Thiol Modification: EGF was first reacted with heterobifunctional NHS-PEG-maleimide and then bound to thiol-modified PDMS.

Using Method 1 (Plasma Modification), 40 to 90 ng/cm^2 of EGF was bound, however 70% of this was adsorbed even under optimized EGF-PEG reaction conditions. Cells rapidly grew to confluence on these surfaces, and cell counts increased significantly compared to control surfaces. Extracellular matrix protein production was also increased on the EGF-modified surfaces, corresponding to significantly higher levels of cell adhesion observed under a detachment force.

Modification by Method 2 (Hydrosilylation) resulted in 10 to 300 ng/cm^2 of bound EGF, of which 20% was adsorbed. However, despite increased EGF binding homogeneity, the cell growth was slower on these surfaces than on those prepared by Method 1, and coverage was non-uniform at all EGF concentrations. This is likely due to a higher underlying PEG density, and binding of the PEG and EGF in clusters on the

surface. Simultaneous tethering of the cell adhesion peptide YIGSR had no further effect on cell coverage.

Using Method 3 (Thiol Modification), 24 to 65 ng/cm^2 of EGF was bound, of which 22% was adsorbed. This method enables more homogeneous EGF surface binding than Method 1, with a lower PEG density than Method 2. However, free thiol groups were inhibitory to corneal epithelial cell growth, even in the presence of bound EGF. Defunctionalization of free thiols by reaction with 3-maleimidopropionic acid restored cell growth and morphology on the PDMS, and may hence allow for retention of the proliferative effect of the EGF.

These results indicate that while tethering of EGF to PDMS can improve the coverage by corneal epithelial cells, and presents a promising strategy for modification of polymeric artificial cornea materials, the effects are highly dependent on the underlying surface chemistry.

Acknowledgements

There are many people who have provided valuable assistance throughout my PhD work that I wish to acknowledge. My supervisor, Dr. Heather Sheardown, has been a tremendous source of inspiration, guidance and encouragement, as well as a positive role model and friend. It has truly been a pleasure to work with her.

I also thank my committee members, Dr. Kim Jones and Dr. Judy West-Mays, for their insightful discussions, advice, and technical assistance with my project.

There are many people within the Sheardown, Jones and Brash labs who have provided not only help with various experimental techniques, but also friendship and a stimulating, enthusiastic environment in which to work. In particular I thank Lina, Laura, Marta, Larry, Derek, Andrew, Alex, Rena, Glenn, Wei, Zhanxu, Sal, Nadira, Dong, Maud, Jennifer, Mark, Meghan, Lindsay, Scott, Emir and Chris. I would like to thank the various other people within the Chemical Engineering department who have assisted me over the years, including Paul Gatt, Gord Slater, Doug Keller, Justyna Derkach, Lynn Falkiner, Kathy Goodram, Julie Birch and Andrea Vickers.

Given the interdisciplinary nature of my research, I was most fortunate to have a network of people within other departments to whom I could turn for guidance and technical help to expand the boundaries of my project. In the Department of Chemistry, assistance provided by Dr. Michael Brook, Dr. Hong Chen, Dr. Jian Guo, Dr. Amro Ragheb, Dr. Yang Chen, Renita D'souza, Lihua Liu and Jill Ranger is greatly appreciated. In the Department of Pathology and Molecular Medicine, I thank Dr. Dhruva Dwivedi and Zahra Nathu for their time and patience in teaching me various techniques.

Additionally, the provision of corneal epithelial cell lines and assistance with seeding procedures by Dr. May Griffith and Cecilia Becceril at the University of Ottawa Eye Institute is gratefully acknowledged.

Finally, I thank my family, whose support was a key component to the success of this project. My parents, Helga and Helmut Klenkler, and brother, Richard, have continually supported me over the years and fostered my desire to learn more and take on new challenges. My husband, Santiago Faucher, has been an infinite source of inspiration, encouragement and understanding, and I know that together, anything is possible. My daughter, Sofia, is my other great accomplishment during my time as a PhD student, and a reminder every day to see the wonderful opportunities that the future holds.

To Santiago and Sofia.

Table of Contents

List of Figures

1.0 LITERATURE REVIEW AND SCOPE OF PROJECT

1.1 Background

Approximately 120 million people worldwide have vision problems due to corneal opacification from injury or disease, and 10 million of those suffer from blindness. Disorders of the cornea are currently second only to cataracts as a cause of vision loss [1]. While the standard treatment by donor graft transplantation has a success rate of over 80% [1], patients afflicted by burns, severe dry eye, immunological disorders, stem cell deficiency, vascularization or ocular diseases such as Stevens-Johnson Syndrome (SJS) and ocular citracial pemphigoid, are often not able to support corneal transplants due to past or ongoing chronic inflammation [2,3]. In some cases of repeated graft rejection, which may also occur for unknown reasons, the success rate of future transplantation drops to near zero [3].

An additional severe limitation to transplantation is the availability of donor organs, which due to longer life expectancies, the growing popularity of refractive surgery, and increasing incidence of infectious disease, is not sufficient to meet the patient requirements; waiting lists exceeding two to five years are now common in North America [1,4,5]. This is also a particular issue in third world countries, where instances of corneal blindness are rising, yet the skills and resources to perform transplant surgeries are limited [4,6]. Hence, a readily available, off the shelf, corneal prosthesis is a desirable alternative for treatment of these patients. However, despite significant progress since the first artificial corneas were developed in the mid-1800s, development of an ideal corneal

prosthesis has remained an elusive goal. Currently, although two devices are in clinical trial stages and other models are being actively researched by various groups, numerous problems and complications remain, and there is no synthetic device in widespread clinical use [1].

1.2 Structure of the Cornea

The cornea is a tough, transparent, avascular membrane forming one sixth of the outer wall of the eye, functioning as the primary optical element and protective barrier for the intraocular contents [2,7]. It is comprised of three distinct cellular layers as shown below in Figure 1-1. The anterior surface consists of five to seven layers of epithelial cells adherent via tight junctions, which maintain barrier function and mediate diffusion of water, oxygen, nutrients and growth factors from the adjacent tear layer [2]. The epithelial cells also secrete a mucin-like glycoprotein which allows for spreading of a smooth tear film over the outer ocular surface [8]. Renewal of the corneal epithelium, a 1- to 2-week process, occurs by proliferation and differentiation of stem cells in the limbus, a 10- to 12-cell layer transitional zone of the cornea [9,10]. The epithelium is organized in a stratified structure, with columnar basal cells, polygonal wing cells and flattened squamous cells at the surface [11]. Mitosis in the basal corneal epithelial layer is followed by differentiation of the resulting daughter cells as they move up to the suprabasal layers, where ultimate apoptosis and sloughing off into the tear layer occurs [2,10].

The stroma forms the main structural element of the cornea, and consists of orthogonal sheets of collagen fibers with interspersed fibroblast-like keratocyte cells [2].

Proteoglycan molecules and associated hydrated glycosaminoglycans maintain the regular spacing between the collagen sheets required for transparency [2]. The innermost layer of the cornea, the endothelium, consists of a single layer of non-proliferating cells, which actively pump excess water out from the stroma into the adjacent aqueous humor, preventing stromal swelling and ensuring corneal clarity [2,10].

The basal epithelial cells are anchored through hemidesmosomes to an underlying basement membrane, which is comprised of adhesion proteins including laminin-1 and type IV collagen [12,13]. Several cellular integrin receptors, particularly containing the α_6 subunit, are located within the hemidesmosome complexes and bind to the matrix proteins to mediate cell adhesion and migration [14]. An acellular basal lamina, Bowman's membrane, is found below the basement membrane between the epithelium and stroma [2,15]. While there is no proven physiological requirement for this layer, it is thought to be maintained by cytokines released from the adjacent cellular layers which influence the relative position of the stromal cells [15].

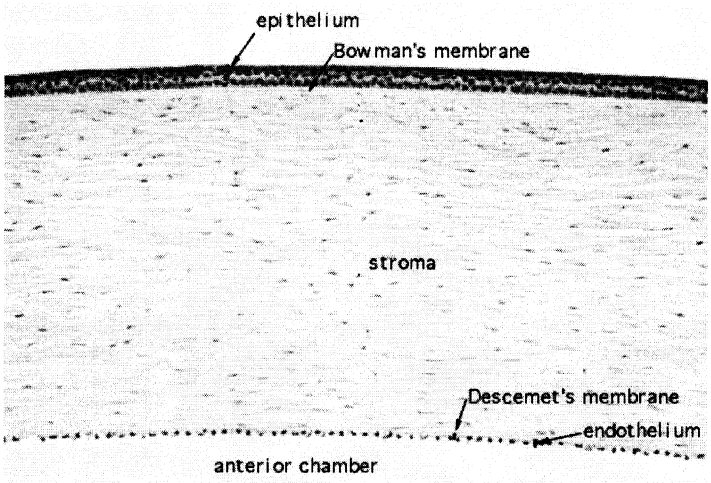

Figure 1-1. Structure of the cornea [16]. Adapted with permission, © 2002, Oxford University Press.

1.3 Artificial Cornea Design Requirements

A polymeric material used for a synthetic keratoprosthesis should satisfy numerous criteria. In addition to transparency and appropriate refractive index, it must have sufficient strength to fulfill the protective barrier function of the cornea and allow for surgical fixation [4]. Biodegradable polymers are generally not suitable due to requirement for transparency and lack of corneal vascularization [2]. The material must be permeable to oxygen and nutrients for survival of the surrounding cells, and should not cause excessive toxic, immune or inflammatory responses which could result in biodegradation, calcification, or tissue melting [4,17]. Fortunately, due to its avascular nature, the cornea is a relatively immune privileged site rendering it an excellent candidate for development of a synthetic prosthesis. Additionally, the presence of transforming growth factor-β (TGFβ) in the fluid of the adjacent aqueous humor assists in induction of immune deviation, and prevention of angiogenesis, in the anterior eye segment [18-20].

The response to the implant material by the different cell layers of the native cornea is a key design consideration, as shown in Figure 1-2. It is generally accepted that the material should be biocompatible, encouraging colonization by host stromal cells for integration into the surrounding tissue and limiting inflammation [4,17]. In light of this, most devices currently in development are based on a "core-and-skirt" type design (Figure 1-3) which is implanted in an intralamellar location, similarly to a penetrating keratoplasty. The device consists of a flexible, transparent, impermeable optical core, joined permanently to a porous, flexible, hydrophilic skirt which enables fibroblast

ingrowth and extracellular matrix deposition in a similar manner to the wound healing process, to anchor the device in the eye [2,4,17].

A further design parameter, which has not been as extensively researched, is the coverage of the anterior implant surface by a confluent layer of corneal epithelial cells. This is thought to improve long-term device integration and stability by enabling tear film spreading, removing the need for external coverage of the skirt material, and preventing bacterial infection and stromal exposure to proteinases and inflammatory cells [2,4,17,21]. While significant advances in keratoprosthesis design have been made in recent years, particularly related to stromal cell anchorage, lack of epithelialization remains a persistent problem. The absence of an epithelial layer can subsequently lead to epithelial downgrowth, a phenomenon in which epithelial cells migrate down the implant periphery rather than over the anterior surface. When this occurs, the exposed stromal collagen at the implant interface is digested by proteolytic enzymes, leading to stromal necrosis (tissue "melting") and eventually to the spontaneous extrusion of the implant from the eye [2,22].

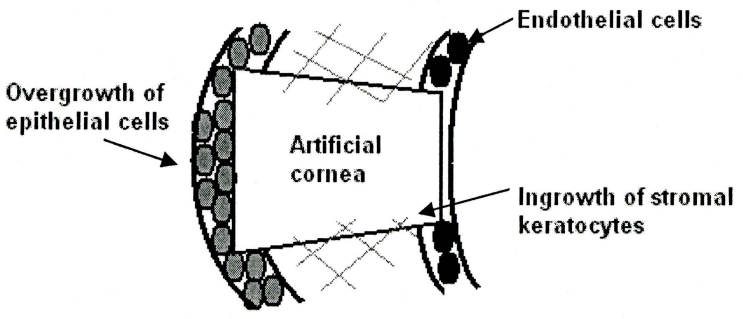

Figure 1-2. A suitable artificial corneal implant requires the ingrowth of stromal keratocytes for anchoring the implant in the host tissue, and the overgrowth of corneal epithelial cells to provide a smooth continuous layer for ocular clarity, protect the underlying structures of the eye and prevent epithelial downgrowth [adapted from 23].

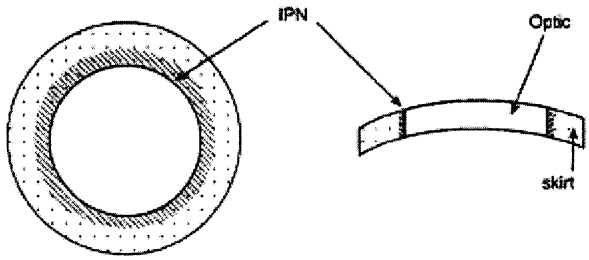

Figure 1-3. Core-and-skirt design for a keratoprosthesis [17]. The transparent optic is surrounded by a porous skirt which allows for cellular colonization. In this model, the optic and skirt components are joined together by an interpenetrating network (IPN). Reproduced with permission, © 2000, Elsevier.

1.4 Artificial Cornea Materials

Despite a wide variety of implant designs and materials, there has been limited success in achieving long-term stability in the eye, and retention of a corneal prosthesis for over 10 years is a rare exception [22]. A number of materials have been investigated for use in both the core and the skirt elements [2,4,6,22,24,25]. While non-integrated polymethylmethacrylate (PMMA) designs, such as the Dohlman-Doane keratoprosthesis, continue to be implanted in clinical studies, serious complications and reversal of visual improvements persist [26]. More recent designs have employed porous polymers which allow for biocolonization by host corneal cells. The model of Trinkaus-Randall et al. consists of a poly vinyl alcohol (PVA) hydrogel optic and skirt of a fibrous polybutylene/polypropylene web [27]. Keratocyte migration and deposition of collagen and glycosaminoglycans as well as production of growth factors in the skirt were detected within weeks of implantation in rabbit corneas, particularly when the web was preseeded with stromal cells [27]. These devices have been found to be stable in rabbit eyes for up to 6 months; neovascularization and edema have been observed but were reduced by

argon plasma treatment of the material [27,28]. Release of fibroblast growth factor (FGF) over three weeks from a calcium/alginate matrix incorporated into the porous skirt led to early detection of vascularization, which is thought to correlate with increased wound strength [27]. The controlled release of growth factors which are active in corneal wound healing, including FGF and TGFβ, to further enhance early fibroplasia and matrix remodeling with minimal neovascularization remains the subject of investigation [27,28].

The BIOKOP design of Legeais consists of a porous expanded polytetrafluoroethylene (PTFE) skirt, fused with a surface-modified polydimethylsiloxane (PDMS) optic. The device is pretreated with serum to render the skirt material hydrophilic [29]. Keratocyte colonization and collagen deposition in the skirt were shown, particularly after pre-seeding the polymer in the presence of various growth factors [30]. Despite promising initial clinical trials [30], recent results have been disappointing with high incidence of corneal melting [31]. The lack of epithelialization of the optic surface may lead to extrusion in some patients and hence prevent long-term success of the implant [29].

The material used for the optic component has also been the subject of investigation, as the historically most commonly used polymer, PMMA, is rigid, hydrophobic, and does not promote epithelial cell attachment [2,22,24]. Hydrogels have several advantages over PMMA, including flexibility and high nutrient permeability due to water contents similar to the native cornea, but must be modified to allow for epithelial cell attachment and have relatively poor mechanical properties [2,32]. PVA hydrogels with high elasticity and tensile strength were synthesized by Trinkaus-Randall [33], and

although surface attachment of extracellular matrix proteins improved epithelialization in vitro, the results under the shear stress of blinking in vivo were less promising [2]. Similarly, the polyvinylpyrrolidone-coated PDMS of Legeais' design, while possessing improved mechanical properties over a previous version with a PMMA optic [34], was not successful in establishing an epithelial layer [29]. More recently, Myung et al. have developed a high-strength, nutrient permeable interpenetrating network of polyethylene glycol (PEG) and a second hydrophilic component such as polyacrylic acid (PAA) [35,36]. This is linked at the periphery to a microperforated poly hydroxyethyl acrylate (PHEA) skirt, and biomolecules may subsequently be tethered to this substrate material; for example, binding of collagen was shown to enhance corneal epithelial cell growth over the optic component *in vitro* [35]. Preliminary *in vivo* testing demonstrated the closure of corneal wounds and coverage of the material by multilayered epithelial cells within two weeks of implantation [36].

The AlphaCor device developed by Chirila et al. has advanced the farthest in terms of clinical usage and is currently approved by the FDA. In this design, the stability of the interface between the core and skirt is optimized by using poly(2-hydroxyethyl methacrylate) (PHEMA) for both the porous skirt (in the form of an opaque sponge) and the optic (a transparent gel); the two components are intimately connected as an interpenetrating network [6]. Several animal studies and clinical trials have been conducted with follow-up ranging up to 77 months, and retention to one year was achieved in over 80% of cases [37-40]. Various ocular complications including stromal melting and poor biointegration were noted, however. In particular, complications due to

calcification and low mechanical strength of the PHEMA sponges have not been resolved to date despite continuing experimentation [17,41]. Also of potential concern is the lack of epithelialization, although it is suggested by this research group that epithelialization of this device is not essential, given the intimate optic-skirt junction and biointegration of the skirt which prevent epithelial downgrowth [17]. Surface modifications of the hydrogel to minimize bacterial adhesion and improve hydrophilicity have been investigated, however [17].

1.5 Epithelialization of Artificial Cornea Materials

It is evident that while progress has been made toward improving design, stromal cell anchorage and bulk mechanical properties of corneal prostheses, the ability of the devices to promote growth of an epithelial layer must be further improved to ensure long-term stability of the implant. The epithelial cells must be able to migrate from the remaining host corneal tissue over the implant surface, attach to the material and proliferate to restore complete coverage and ultimately form a self-renewing epithelial layer [21].

1.5.1 Material Surface Properties and Corneal Epithelial Cell Growth

Several factors including surface hydrophilicity, chemistry, porosity, topography and permeability to nutrients have been shown to affect epithelialization, particularly in *in vivo* environments. Importantly, as the initial response to a synthetic implant is typically adsorption of proteins from the surrounding fluid, the nature of the adsorbed protein layer, which is highly dependent on surface chemistry, charge and hydrophilicity,

plays a key role in dictating the subsequent cellular response [42-46]. Proteins produced endogenously by the cells themselves may also adsorb to the substrate, and mediate cell adhesion and migration if present in an active conformation [43]. While highly hydrophobic substrates are generally thought to cause denaturation of adsorbed proteins and inhibit cell and tissue growth [42,43], overall a basic relationship between properties such as surface wettability and cell adhesion remains difficult to establish and varies with cell type and experimental conditions [44]. Certain hydrophobic materials, such as perfluoropolyethers (PFPEs), are able to support epithelial cell growth *in vitro* [47].

Surface chemistry and charge were shown to be critical factors in a study by Chan *et al.* [42], where only intermediate surface concentrations of a zwitterion additive supported corneal epithelial cell growth, likely due to enhanced fibronectin adsorption under these conditions. HEMA hydrogels prepared by Wu *et al.* [14] supported corneal epithelial cell adhesion and actin filament formation when surface-modified with amines, but not with carboxyl moieties. Latkany *et al.* [48] observed that surface oxidation of PVA with argon plasma improved cell adhesion under shear force in organ culture studies. Acetone and ammonia plasma treatment of PVA had no effect, however, and other in vitro studies of argon-treated PDMS surfaces by Hsuie *et al.* show lack of cell colonization [49]. George and Pitt [21] and Hsiue *et al.* [49] compared corneal epithelial cell mitotic rates on various polymeric materials and plasma surface treatments in culture, and found the highest growth on PDMS modified with plasma polymerized PHEMA at low graft densities. However at high PHEMA density, the growth was inhibited, similarly to unmodified PHEMA devices [2,50]. Cell migration is also influenced by surface

properties, as shown by Steele *et al.*, who observed a linear increase in migration with wettability, but a reduction in migration on hydrophilic substrates with a mobile surface chemistry [51].

Several experiments have also demonstrated the effect of physical surface structure on epithelial cell coverage. Porosity is an important implant material property, enabling cellular ingrowth and nutrient flux as well as guiding tissue movement and enhancing formation of adhesion complexes [51]. Individual epithelial cells and larger colonies have been demonstrated to migrate along track etched polycarbonate, polyurethane and silicon substrates with similar size and density of pores or grooves to those reported within the native corneal basement membrane (on the order of 0.1 μm), although surface chemistry also influences the effect of topography on migration [51,52]. Work in Murphy's lab [53] demonstrated that increased adhesion under shear stress was associated with nanoscale versus microscale grooves and holes, due to enhanced cell-substrate interactions at surface discontinuities. Introduction of such small pores also appears to be conducive to extracellular matrix (ECM) protein deposition and proper stratification of the resulting epithelial cell layer [11]. Larger pores reduced or halted adhesion, migration and stratification, indicating that surface topography has a significant effect on epithelialization and excessive roughness may in fact inhibit this process [54,55]. Proliferation of corneal epithelial cells, however, decreased with nanoscale feature size on polyurethane and silicon substrates [56]. These observations indicate that nanosized features within the basement membrane *in vivo* may be involved in controlling cell fate from a more proliferative to a more differentiated state [56], and it is likely that

an optimal combination of surface chemical and physical properties is required to most effectively promote healing and the formation of a confluent epithelial cell layer [51].

1.5.2 Corneal Wound Healing

An alternative, more biologically based approach towards promotion of epithelialization of a synthetic implant is to mimic or use elements present within the natural corneal wound healing process. Injury to the cornea results in a cascade of processes regulated by combinations of growth factors and cytokines; these proteins integrate cellular proliferation, migration, differentiation, apoptosis and intercellular communication, leading to proper tissue restoration and the ultimate restoration of vision. Within minutes after injury, secretion of cytokines by injured epithelial leads to increased growth factor expression in the epithelium and stroma [57,58]. Elevated production of keratinocyte growth factor (KGF), hepatocyte growth factor (HGF), platelet-derived growth factor (PDGF) and epidermal growth factor (EGF) by cells of the cornea and lacrimal gland occurs for more than seven days post-injury. These factors act to stimulate epithelial cell proliferation and migration, which begins within hours after the injury to restore barrier function over the wound [58,59]. Increased expression and activation of the associated growth factor receptors also occurs throughout the basal epithelial cells of the cornea and limbus [60]. Upon receptor activation, the epithelium is triggered to further produce EGF receptor ligands in an autocrine manner to propagate the initial wound healing response [60].

While limbal cells proliferate in response to EGF [61,62] and KGF [63] in particular, detached epithelial cells at the wound periphery are induced to migrate by HGF [63] and EGF [9,64] on a provisional fibronectin matrix which accumulates at the injury site [65]. Fibronectin is not present in normal epithelial basement membrane, but is detectable within 8 hours of wounding [12]. It is thought that endogenously produced fibronectin, synthesized by wounded corneal epithelial cells, promotes cell adhesion [66]. Fibronectin molecules in tears also promote epithelial cell attachment and migration, and secretion of proteases, such as plasmin (in tears) allows for breaking and reforming of integrin-matrix attachments enabling epithelial cell migration [67]. Topical application of stimulatory growth factors, such as EGF and KGF, has been found to accelerate the epithelial wound healing process in several studies [62,68,69]. Once confluence is achieved over the wound, the cells are triggered to proliferate and eventually differentiate to form a normal stratified epithelium [9,64]. At this point the fibronectin matrix disappears and the normal basement membrane composition of collagen and laminin is restored by cellular protein deposition and remodeling [9].

Stromal keratocyte proliferation begins within 12 to 24 hours after wounding and continues for several days after the injury [58]. PDGF and TGFβ released by the epithelium stimulate stromal cell proliferation and migration, and along with EGF, inhibit fibroblast apoptosis [58,70-72]. Quiescent keratocytes are activated by wounding to differentiate into migratory fibroblasts and myofibroblasts, which are characterized by expression of α-smooth muscle actin, and increased production of growth factors, collagen and matrix metalloproteinases for epithelial healing and stromal remodeling

[58,70,73]. Also, beginning at 12 to 24 hours post-injury, an influx of inflammatory cells into the cornea from the limbal blood vessels and possibly the tear film occurs [58]. Cytokines released from the injured epithelium bind to receptors on keratocytes, which stimulate production of factors chemotactic to inflammatory cells [58,61,74]. These inflammatory cells function to remove pathogens and debris from apoptotic cells [58], and to release PDGF which mediates the wound healing process [63]. Mechanisms within the anterior eye, referred to as anterior chamber associated immune deviation (ACAID), exist to ensure that the response to antigens is devoid of T cells that mediate delayed hypersensitivity and antibodies that fix complement. This enables the central cornea to avoid prolonged immunogenic inflammation which may cause blindness [19,20].

In the weeks to months following the injury and healing of the wound, the cornea returns to a normal state through elimination of inflammatory and myofibroblast/ fibroblast cells, and restoration of a quiescent stroma [58]. Expression of growth factor receptors and proteins returns to pre-wounding levels [59]. Remodeling of the collagen matrix of the stroma also takes place to clear scar tissue, and the epithelium returns to a normal thickness [58].

1.5.3 Extracellular Matrix Proteins

Attempts have been previously made to surface modify polymeric materials with various extracellular matrix (ECM) proteins, including collagen and laminin, which mimic the epithelial basement membrane and have been shown to promote cell adhesion and outgrowth in vitro, and fibronectin, which forms a provisional matrix for cell

migration during wound healing as described above [4,47,75]. It has been suggested that signals from matrix proteins present on an implant surface may trigger migrating cells to reform a basement membrane by ECM protein secretion and formation of adhesion complexes at the surface [75]. Corneal epithelial cells are particularly well-known to synthesize their own matrix proteins compared to other cell types, enabling them to adhere to substrates under a variety of culture conditions [76].

Kobayashi and Ikada [32] covalently bound collagen and fibronectin to PVA hydrogels, observing promising *in vitro* stimulation of epithelial cell coverage. However, when implanted *in vivo*, epithelial downgrowth and device extrusion occurred within 3 weeks [22]. Coating of porous PFPE corneal onlays with a thin layer of collagen I resulted in matrix deposition and epithelialization for up to 39 days in a small sample of feline corneas, and did not interfere with nutritional permeability of the polymer [47]. Myung *et al.* [35] achieved corneal epithelial cell growth *in vitro* on PEG/PAA hydrogels, which typically do not support protein and cell attachment, by covalent tethering of collagen on the material surface. In another study by Sweeney *et al.*, coatings of collagens I and IV and laminin on porous polycarbonate membranes enhanced migration, integrin expression and persistent attachment of epithelial cells in the feline cornea up to nine weeks post implantation [75]. It was noted that more rapid wound closure with other matrix protein coatings did not result in the most persistent epithelial coverage, indicating that cell adhesion may be more critical than migration rate for effective wound healing [75].

While some ECM protein-modified surfaces have shown encouraging results in stimulating epithelialization *in vitro*, early results from *in vivo* testing have been less conclusive, and long-term data are generally lacking [47,77]. In particular, the effects of proteolytic activity on the modified surfaces *in vivo* must be further investigated; fibronectin and collagen are especially susceptible to degradation by proteases on the corneal surface [75,77].

One alternative is the binding of the more stable associated peptide fragments responsible for cellular adhesion, rather than the protein itself. This approach also avoids inflammation potentially associated with the use of animal tissue-derived proteins, as well as increases surface densities for binding to cellular receptors. Corneal epithelial cell growth and adhesion strength to poly(HEMA-co-methacrylic acid) hydrogel substrates *in vitro* were significantly enhanced by tethering of laminin or fibronectin adhesion promoting peptide (FAP) via flexible PEG chains, more so than by tethering of fibronectin or simple coating of the surface with matrix proteins. [77,78]. In several other studies [50,79,80], modification with fibronectin- and particularly laminin-based adhesion peptides (RGD and YIGSR, respectively) was observed to improve epithelial cell adhesion to pHEMA, PDMS and even collagen surfaces *in vitro*. Investigation of several peptide-modified pHEMA surfaces by Merrett *et al.* indicated that YIGSR, at low surface densities, was most effective in promotion of corneal epithelial cell growth, although the peptide immobilization reaction conditions had significant effects on cell spreading and density [50]. Aucoin *et al.* found that combinations of RGD and YIGSR peptides had the greatest stimulatory effect on corneal epithelial cell growth over PDMS

substrates, even in serum-free medium, potentially by more closely mimicking the natural composition of the extracellular matrix [79]. The type of substrate material appears to have an effect on the activity of the matrix proteins or peptides; for example coating of tissue culture polystyrene with various peptide sequences was more effective in promoting cell confluence than coating of hydrogels in the same manner [77], and peptide-modified PDMS substrates were better able to support epithelial cell growth than peptide-modified PHEMA [79].

1.5.4 Growth Factors

An alternate, less investigated method of promoting epithelial cell growth on synthetic materials is through the use of growth factors. Growth factors are soluble peptides produced naturally by many cell types, which promote or in some cases inhibit cellular proliferation, migration and survival [81]. Action may be through autocrine (produced by and acts on same cell type), juxtacrine (acts on neighbouring cell), or most commonly, paracrine (produced by and acts on different cell types) mechanisms [82]. The corresponding cell surface receptors are transmembrane glycoproteins belonging to either the receptor tyrosine kinase (RTK) or G-protein-coupled receptor (GPCR) families [83]. Growth factor binding to an associated receptor leads to a cascade of reactions, often initiating transition to the DNA synthesis (S) phase and ensuing cellular proliferation [81]. Receptor activation may also lead to phosphorylation of Akt, a kinase involved in antiapoptotic signaling [72], and alteration of cell morphology and motility through association with the actin cytoskeleton. However, these events are not common

to all growth factors [81,84] and there is a complex interplay between different growth factors to facilitate wound healing and other processes.

The relationship between growth factor signaling and specific cellular response is not yet well understood. Through studies of human fibroblasts stimulated by epidermal growth factor, it has been shown that a direct relationship between cellular proliferation and growth factor-receptor complex number exists and that EGF (and likely other growth factors) must occupy the receptor for approximately 6 to 8 hours, the time span for cell cycle progression [82]. However it is also thought that an initial 30- to 60-minute signaling phase is required for most growth factors to engage the cell cycle program [81]. At a certain occupancy level where maximum response is achieved, endocytosis of receptor-ligand complexes occurs rapidly; receptors may then either be recycled to the plasma membrane, or proteolysed leading to downregulation of available surface receptors [82,83,85]. As such, the dose-response curve for growth factors may often be non-linear or bell-shaped (Figure 1-4) [82]. Growth-factor induced signaling leading to proliferation may occur at both the plasma membrane [86,87] and by preserved ligand-receptor complexes in intracellular endosomal compartments [83]. Hence, complex internalization to the cell nucleus may not be required for the associated cellular response to be achieved.

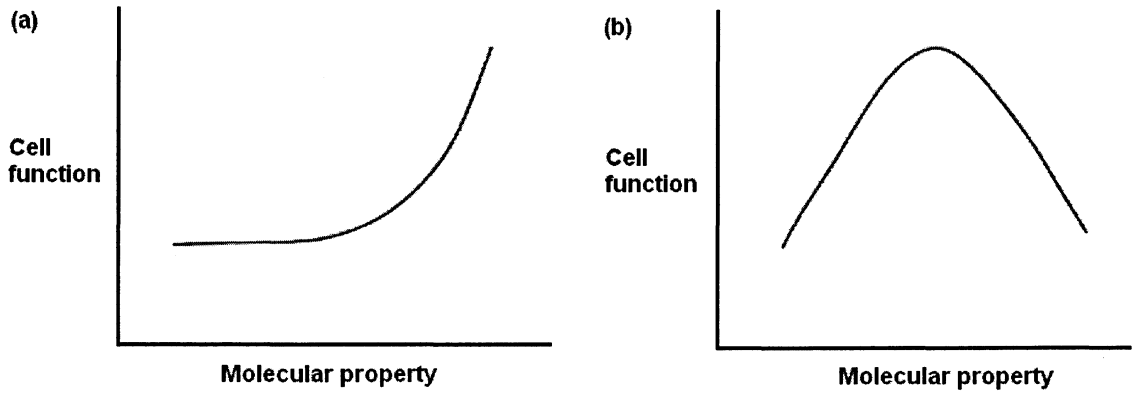

Figure 1-4. Schematic relationship between a cell function and molecular property, such as growth factor concentration. The cellular response may not simply be an increasing or decreasing function of molecular property [adapted from 82].

The effect of growth factors on a cell type may also vary significantly depending on the extracellular environment. Binding of growth factors to the ECM, leading to sequestration or controlled release, may regulate or enhance their effect [88]. On cell binding to the ECM, integrin signaling, shape and cytoskeletal tension, all of which control cell cycle progression triggered by growth factors, are altered [81]. Stimulation by growth factors induces cells to produce or alter the surrounding matrix [89], and promotes migration on the ECM through enhanced integrin expression, affinity or cytoskeletal interactions [65]. In addition, the presence of multiple growth factors may lead to varying responses based on relative concentrations [69].

Understanding the production and function of growth factors in ophthalmic tissues will lead to improved insights into cellular homeostatic mechanisms as well as the wound healing process, which the response over a synthetic implant is desired to emulate. In the cornea, a variety of growth factors produced by the three cellular types regulate cellular proliferation, differentiation, motility and apoptosis in tissue maintenance and

wound healing [69], and hence present promising opportunities for application in a keratoprosthesis design.

1.6 Epidermal Growth Factor (EGF)

Epidermal growth factor (EGF) is of particular interest for use in an artificial cornea application, as it is a well-known, potent mitogen and motogen for epithelial cells including those of the cornea [85]. EGF binds to both low and high affinity sites on cells expressing the EGF receptor (EGFR) [90]. Ligand binding to the EGFR and subsequent receptor dimerization activates receptor tyrosine kinase activity, leading initially to increased active transport of nutrients and, within 8 to 15 hours, increased production of ECM molecules including fibronectin and glycoproteins, DNA synthesis and cellular proliferation unrestricted by contact inhibition [85,90]. Studies have shown that maximal stimulation of DNA synthesis occurs at a concentration of EGF yielding only 25% of maximal receptor binding [85]. EGF receptor phosphorylation also causes actin cytoskeletal rearrangement, promoting cell motility. The simultaneous presence of ECM molecules, such as fibronectin, enhances polarization required for directional migration and facilitates cross-talk between integrins and EGFRs at the leading edge [65,90].

1.6.1 Structure and Properties of EGF

EGF is one of the most highly stable, well-characterized and biologically potent growth factors known to date. It is a compact, globular, water-soluble, 6 kDa polypeptide, comprised of a single chain of 53 amino acids [85,91,92]. The primary structure of mouse

EGF, to which EGF has 70 percent sequence homology, is shown in Figure 1-5a, and the three dimensional structure of human EGF is illustrated in Figure 1-5b. EGF has an isoelectric point of 4.6 [93], and is therefore negatively charged at physiological pH. Studies have shown EGF to retain over 80% of its native structure in PBS at room temperature for 10 days [94]. Three disulfide bonds maintain its three dimensional structure and are required for its biological activity [85]. Of interest for bioconjugation purposes, human EGF contains two lysine residues (Lys28 and Lys48), as well as the N-terminal amine, all of which are exposed on the surface of the molecule [91]. The two critical residues for binding to the corresponding cellular EGF receptor, Arg41 and Leu47, are located in the carboxy-terminal domain and are far from the N-terminus and Lys28 residues [91,95]. Other studies of EGF degradation products suggest that a cluster of aromatic residues containing Asp11, Trp49 and Trp50 are in proximity to each other in the tertiary structure, and are also important for receptor binding [94].

a) b)

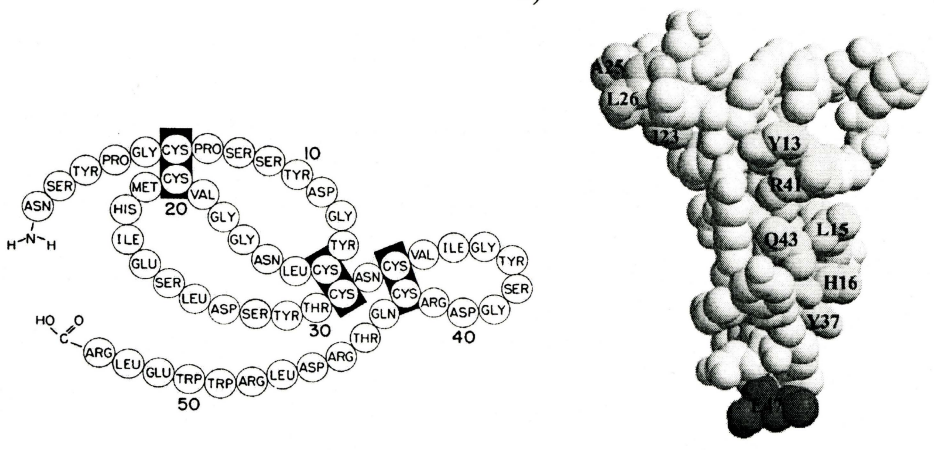

Figure 1-5. a) Primary [85] and (b) space-filling [96] structure of epidermal growth factor. Some of the surface residues thought to be important for receptor binding are shown. Reproduced with permission, © 1979, Annual Reviews www.annualreviews.org, and © 2001, American Society for Biochemistry and Molecular Biology.

1.6.2 EGF in the Cornea

Both high- and low-affinity EGF receptors are found in corneal epithelial cells, particularly in the limbal region and in corneal endothelial cells [62]. Lower levels of low-affinity receptors only exist on stromal keratocytes [59,69]. EGF mRNA has been detected in all three corneal cell types [59], and immunohistochemical staining revealed the presence of the protein in the epithelium, with higher concentrations in the superficial layers, the endothelium, and to a lower extent the stroma [97]. These findings indicate that EGF affects corneal cells in an autocrine, paracrine or possibly juxtacrine manner [62]. The presence of EGF in the lacrimal gland and in tears at concentrations of 0.7 to 9.7 ng/mL likely also contributes to its effects on the corneal epithelium [62,98]. EGF has been associated with vascularization in the cornea in some literature studies; however in other studies no effect was observed [99,100]. The stimulation of angiogenesis by EGF may be linked to its combined presence with or upregulation of other growth factors, particularly fibroblast growth factor and vascular endothelial growth factor (VEGF), during wound healing [101,102].

EGF has been found to inhibit terminal differentiation of corneal epithelial cells and to increase proliferation in a dose-dependent manner at concentrations greater than 0.1 ng/mL *in vitro* [59,69,103]. However, in some studies concentrations exceeding approximately 10 ng/mL were found to decrease cell proliferation and cell numbers [69,103,104], indicating a biphasic response to this growth factor. *In vivo*, it has been reported that the topical application of EGF at concentrations of between 10 and 20 μg/mL, and continuous perfusion at 50 μg/mL, can improve the rates of healing of

corneal wounds [68,105] It is likely that autocrine and lacrimal gland production of this growth factor plays a role in maintenance of normal corneal epithelial thickness [62].

EGF is also a potent stimulator of corneal epithelial cell motility *in vitro* in regions of low cell density at concentrations of 10 to 50 ng/mL [64,106], and is particularly important for enabling ECM interactions and haptotactic migration on a fibronectin substrate [65]. Similar effects are noted in organ culture systems, where a dose-dependent stimulatory effect on migration was seen at EGF concentrations up to 10 ng/mL [107,108], and *in vivo* [60]. EGF upregulates expression and activation of β_4 integrins, and enhances degradation and reformation of hemidesmosomes in epithelial cell migration following injury [109,110]. Endothelial cell proliferation is similarly stimulated by EGF in culture, with a plateau in response at concentrations of approximately 10 ng/mL [69,103]. Proliferation is further enhanced by the addition of ECM molecules [111]. The weak effect of EGF observed on stromal cell growth is consistent with the presence of only low-affinity EGF receptors on this cell type [69,103].

1.7 EGF Tethering to an Implant Surface

In order to harness the biological potency of growth factors such as EGF for directing cellular response to a biomaterial device, a suitable method for delivery to the surrounding cells is required. Delivery of growth factors may be achieved through various means, including from solution, by controlled release devices, and by adsorption or chemical immobilization to the implant surface. The mechanism of delivery must allow for sufficient presence of the drug at the target location, as the growth factor must

occupy the receptor for a sufficient length of time to effect cell cycle progression as described previously [81,82]. Immobilization of the protein is expected to result in improved control over local drug concentration versus delivery in a soluble form, because diffusive and degradative losses are limited. Growth factor internalization and receptor downregulation within the cells, which occurs at a maximal level of ligand occupancy [82], is also thought to be limited by this method [86,87].

Surface immobilization must however be performed in a manner such that the receptor binding and resulting biological activity of the growth factor is preserved. In a key study [86], Kuhl and Griffith-Cima showed that EGF tethered to glass substrates via PEG spacer chains retained its activity in promoting DNA synthesis in rat hepatocytes. Use of growth factor immobilization techniques depends on the assumption that signaling at the plasma membrane, without internalization into the nucleus, is sufficient to initiate cell proliferation. This mechanism may resemble the juxtacrine signaling of membrane-anchored growth factors, which deliver intercellular signals while adhesive interactions between cells are maintained [87]. Although unproven in wild-type cells, this assumption is supported by the study by Kuhl and other examples of growth factor tethering mentioned below. Additionally, previous experiments with fibroblasts expressing internalization-deficient EGF receptor, in which EGF elicited a normal mitogenic response at significantly lower concentrations than in wild-type cells, imply that receptor activation at the cell membrane is sufficient for signaling [112].

Gobin and West [113] observed that EGF bound to PEG diacrylate hydrogels maintained mitogenic activity and promoted migration of fibroblasts. Other experiments

with TGFβ tethered via PEG to fibrillar collagen [114] and bound to PEG hydrogels [115] also achieved improved growth factor activity versus delivery in soluble form. Ito et al. demonstrated activity of EGF and insulin covalently bound directly to polymer surfaces, with cell growth further enhanced by co-immobilization of ECM proteins [87,116]. VEGF [117,118], TGFβ [119], FGF [120], nerve growth factor (NGF) [121] and bone morphogenic protein (BMP) [122] have all been successfully tethered to materials to promote growth and migration of various cell types. Tethering of extracellular matrix proteins and associated peptides has also been extensively used to enhance cell spreading and adhesion on biomaterials as previously described in section 1.3.3 [35,77,123].

It is further hypothesized that once the cells adhere to a substrate and the tethered protein elicits its initial response, the cells subsequently produce their own extracellular matrix and growth factors to create the optimal environment for their survival [77]. For example, Mann *et al.* observed that tethering of TGFβ stimulated extracellular matrix protein production by vascular smooth muscle cells [115], and Liu *et al.* detected increased collagen and bone production by mesenchymal stem cells in poly(lactide-co-glycolide) (PLG) scaffolds where BMP was tethered [122].

Use of a polymer spacer such as PEG between the growth factor and the surface (Figure 6), as in many of these studies, is believed to enhance the steric accessibility of the growth factor for binding to cellular receptors. The increased flexibility imparted by the presence of the polymer chain may be important for receptor mobility within the cell membrane and dimerization needed for subsequent intercellular signaling [86].

PEGylation of bioactive molecules has been shown to lead to improved water solubility and stability, and reduced immunogenicity, *in vivo* [114,124].

PEG-tethered EGF was shown to result in significantly increased mitogenic activity over EGF adsorbed directly to a material surface [86], likely because adsorption results in denaturation or protein conformations inaccessible to cellular receptors. RGD peptides were also more active in promoting cell spreading on PEG diacrylate hydrogels when tethered with a PEG spacer arm versus without [123]. Further, as PEG is well known to be highly hydrophilic and protein repulsive [125], it is thought that non-specific adsorption of other proteins from the surrounding fluids may be reduced on PEG-containing surfaces depending on the density of PEG bound [126]. This was demonstrated by Myung *et al.* [35], who did not observe collagen adsorption or cell adhesion on PEG/PAA hydrogels; when the PEG was functionalized and collagen covalently tethered to the hydrogel, epithelialization ensued.

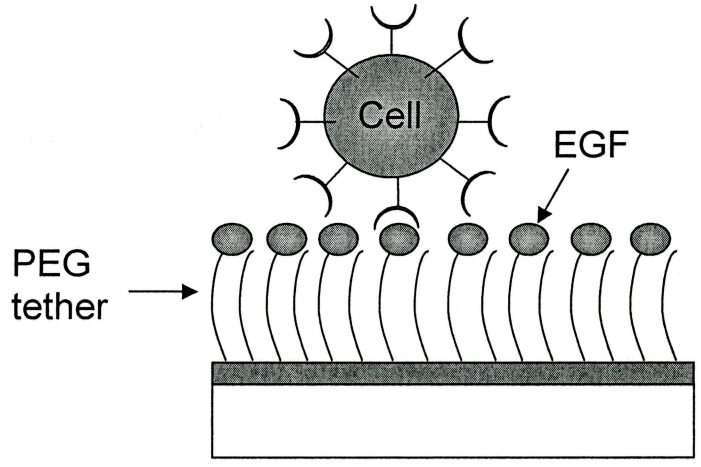

Figure 1-6. Tethering of epidermal growth factor to a substrate material via flexible polyethylene glycol chains. The growth factor binds to receptors on the cell membrane where signal transduction is thought to occur [adapted from 87].

The effects of tethered growth factors such as EGF on cell proliferation, migration and adhesion may be dependent on cell type and the presence of other factors such as serum or ECM proteins. For example, in the study of tethered EGF by Kuhl and Griffith-Cima, ECM proteins were also pre-adsorbed to the surface [86], and in the work by Gobin and West, polymer matrices contained bound RGD in addition to EGF [113]. Other studies [50,77] also indicate that serum is present in the culture medium, which will presumably lead to the adsorption of proteins and alteration of the cellular response to the bound bioactive molecules. It would be of significant interest to determine the effect of the tethered EGF alone on these parameters, as well as the importance of EGF concentration in this surface-bound form. Few literature studies to date have examined the effect of bound growth factor concentration on cellular response, which is known to be a key factor for exposure in the soluble form as discussed previously. Concentration gradients of immobilized NGF [121] and FGF [120] elicited preferential outgrowth and migration of neurite and vascular smooth muscle cells, respectively. Zisch *et al.*, however, found a biphasic dose response in endothelial cell proliferation with concentration of VEGF incorporated into fibrin matrices [117].

1.7.1 PEG Tethering Chemistry

The chemistry used for tethering of the growth factor is also an important factor in determining the amount and activity of bound protein. For many proteins, particularly those that do not contain free reactive thiol groups (including EGF), tethering to PEG is most commonly accomplished using an activated PEG with functional groups able to

bind to free amines within lysine and N-terminal amino acid groups. Active N-hydroxysuccinimidyl (NHS) esters of PEG carboxylic acids are the most frequently used acylating agents for protein modification, and react with primary amines at near physiological conditions to form stable amides as shown in Figure 1-7 [124,127]. One issue with this pegylation method is the susceptibility of the succinimidyl ester group to hydrolysis; it has been found that increasing the distance between the active ester and the PEG backbone significantly increases the hydrolysis half-life, and these modified PEG active esters are therefore preferably used [124].

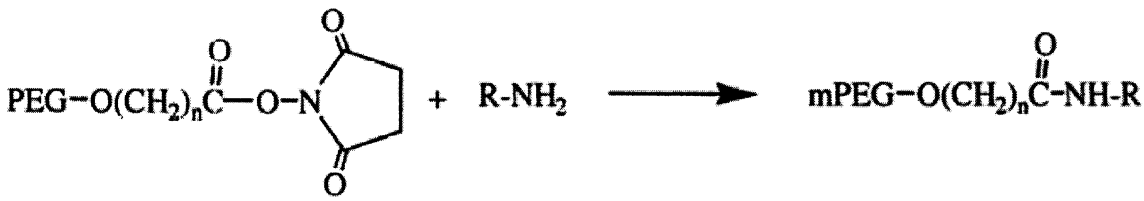

Figure 1-7. Reaction of PEG NHS ester with primary amine on a protein [124].

In previous studies growth factors have been tethered to a surface via a homobifunctional PEG spacer, using either a surface-first or solution-first reaction scheme (where the PEG is bound first to the surface or to the protein, respectively) [86,114,119]. Use of a solution-first scheme may prevent simultaneous adsorption (and denaturation) of non-pegylated protein to the surface, as indicated by the results of Kuhl and Griffith-Cima [86]. However, the yield of the PEG-protein binding reaction and competing reactions with the functional groups on the PEG (e.g. hydrolysis) must be considered to maximize covalent binding and growth factor activity, and have not been

extensively addressed in the literature. Several other recent studies have utilized heterobifunctional PEGs for tethering of proteins, by incorporation of the pegylated protein onto PEG and other hydrogel scaffolds [35,113,115,120,122]. Selection of appropriate functional groups on the PEG may enable greater control over the PEG-protein binding reaction and the composition of the modified surface. Both methods are analyzed in this work in order to determine the optimal surface properties for stimulation of epithelial cell growth by tethered EGF.

1.8 Scope of Work

The overall objective of this work is to develop a polymeric material which actively promotes the growth and adhesion of corneal epithelial cells, for use as the optic component of a keratoprosthesis and more generally to better understand the interactions between corneal epithelial cells and synthetic materials. Polydimethylsiloxane (PDMS) has been chosen as the substrate material, due to its proven ophthalmic compatibility, transparency, oxygen permeability and mechanical strength [4]. Additionally, it has been shown to have the potential to be modified to enable nutrient permeability similar to that of the natural cornea [128]. However, PDMS is highly hydrophobic and even with this modification, does not, on its own, support the growth of a confluent epithelial cell layer on its surface.

The potential of EGF to mediate epithelialization in the native cornea raises interesting possibilities for its use in promoting epithelial cell growth over a synthetic corneal implant. It is hypothesized in this work that localization of EGF to the surface of

a PDMS corneal prosthesis should be effective in promoting epithelial cell coverage of the device, through direct promotion of cell proliferation on the material similarly to the corneal wound healing process. The increased overall extracellular matrix deposition by the cells on the surfaces should thus also improve cellular adhesion to the polymer. This strategy may provide further stimulation of epithelialization than the use of material surface properties or ECM adhesion proteins alone, as has been previously attempted. It is anticipated that the results from this work may also be extended to additional substrate materials.

EGF is tethered to PDMS substrates via polyethylene glycol (PEG) chains, as this is expected to retain the maximum growth factor biological activity. As PDMS does not contain any reactive functional groups, it must be surface-modified to enable subsequent tethering of a growth factor. Three different tethering methods are characterized in this work (shown in Figure 1-8), and the effects of tethering chemistry and bound EGF concentration on corneal epithelial cell growth are analyzed to develop an optimal surface modification scheme.

1.8.1 "Solution-First" Method (Plasma-Modified Surfaces)

In this method (Figure 1-8a), reactive amine functional groups are introduced to the PDMS surface by first depositing an allylamine plasma polymer layer. EGF is then reacted in aqueous solution with an excess of homobifunctional N-hydroxysuccinimide $(NHS)_2PEG$ derivative. The aminated substrates are exposed to the resulting reaction mixture to bind the pegylated EGF via the free remaining NHS group on the PEG. By

varying the ratio of EGF to PEG in solution, a range of EGF and PEG surface concentrations can be attained. Results from these surfaces are contained in Papers 1 to 3 (Chapters 4 to 6).

1.8.2 "Surface-First" Method (Hydrosilylation Surfaces)

In this second method (Figure 1-8b), PDMS is first modified by introduction of reactive SiH groups at the surface, which are subsequently reacted by hydrosilylation with the allyl group of a heterobifunctional allyl-PEG-NHS [129]. This method results in a high-density functionalized PEG layer which can be subsequently used for the generic binding of biomolecules of interest, and which limits adsorption of free protein between PEG chains [130,131]. Two variations of this method are used: a) the "direct" method, where allyl-PEG-NHS is bound directly to the PDMS, and b) the "indirect" method, where allyl-PEG-OH is first bound and subsequently converted to allyl-PEG-NHS. The "indirect" method circumvents issues with the instability and difficult synthesis of allyl-PEG-NHS, and is expected to yield the same surface chemistry as the "direct" method.

Upon exposure of the PEG-modified surfaces to an EGF solution, the EGF is then attached via the free NHS group on the surface-bound PEG. Use of a heterobifunctional PEG in this scheme is expected to provide improved control over EGF binding versus the "solution-first" plasma-modification technique, by limiting multi-pegylation of the EGF, the competing hydrolysis reaction on the free NHS group of the PEG, and associated non-specific EGF adsorption. By varying the EGF solution concentration, a range of EGF

surface concentrations can be achieved. Results from these surfaces are presented in Papers 4 and 5 (Chapters 7 and 8).

1.8.3 "Heterobifunctional PEG Solution-First" Method (Thiol-Modified Surfaces)

This third reaction scheme (Figure 1-8c) combines features of the two previous methods, including improved EGF binding control afforded by a heterobifunctional PEG, and a solution-first approach to control the amount of PEG binding to the surface. PDMS is first modified with 3-mercaptopropyltrimethoxysilane (MPS) to introduce reactive SH (thiol) groups at the surface. EGF is then reacted in solution with a heterobifunctional NHS-PEG-maleimide. Reaction via the NHS group leaves the maleimide group, which is relatively more stable in aqueous solution, free to subsequently bind to the thiol groups on the PDMS surface.

Maleimides are desirable for use in tethering reactions due their good stability in aqueous environments and their selective and efficient reactivity toward thiol groups [132]. It is thought that using this chemistry, the reaction between EGF and PEG in solution can be carried for longer time periods, without a competing reaction for the free maleimide functional group. This is expected to further limit the amount of unreacted EGF which can subsequently adsorb to the surface rather than covalently bind. Surfaces generated by this method should hence be more homogeneous than the initial surfaces prepared by scheme 1.8.1 (Plasma Modification), with a lower PEG density than those prepared by scheme 1.8.2 (Hydrosilylation). Results from these surfaces are detailed in Paper 6 (Chapter 9).

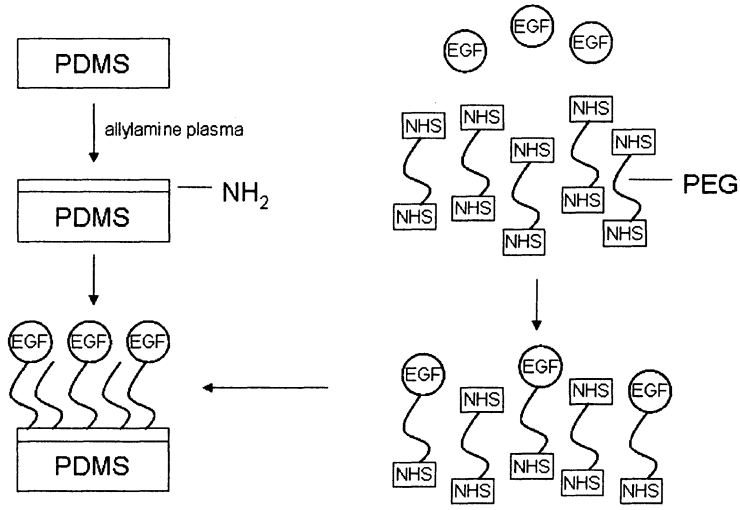

Figure 1-8a. Binding of EGF to PDMS via Method 1 ("Plasma Modification").

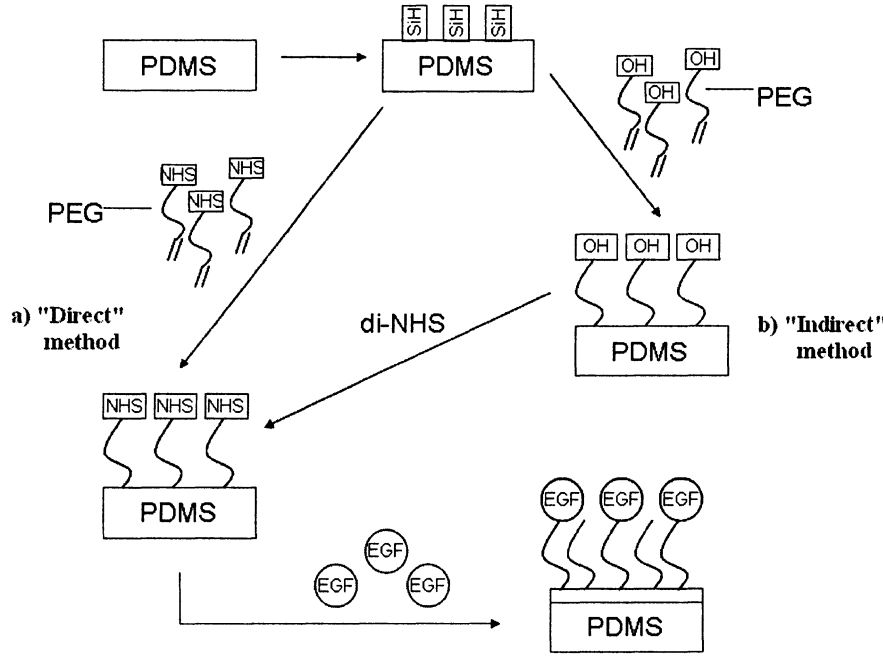

Figure 1-8b. Binding of EGF to PDMS by Method 2 ("Hydrosilylation"). Both variations used to prepare these surfaces ("direct" and "indirect") are shown.

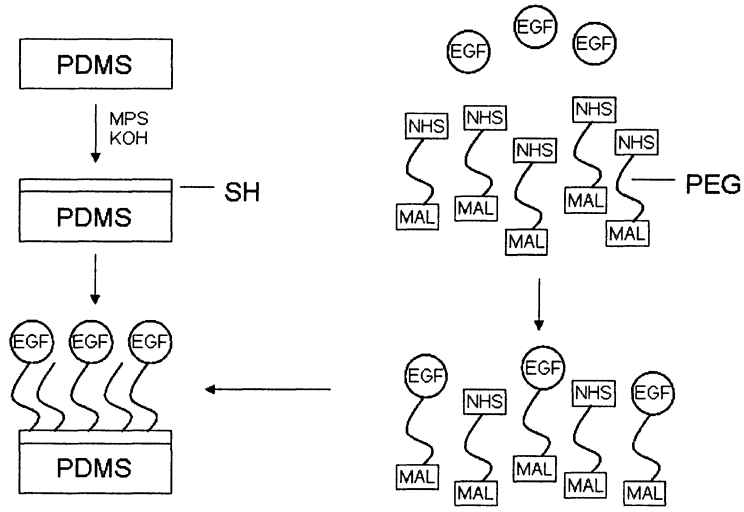

Figure 1-8c. Binding of EGF to PDMS by Method 3 ("Thiol Modification").

1.9 References

1. Carlsson DJ, Li F, Shimmura S, Griffith M. Bioengineered corneas: How close are we? Curr Opin Ophthalmol 2003; 14:192-7.

2. Trinkaus-Randall V. Cornea. In: Lanza RP, Langer R, Vacanti J (Eds). Principles of Tissue Engineering (Second Edition). San Diego: Academic Press, 2000. p. 471-91.

3. Khan B, Dudenhoefer EJ, Dohlman CH. Keratoprosthesis: An update. Curr Opin Ophthalmol 2001; 12:282-7.

4. Griffith M, Hakim M, Shimmura S, Watsky MA, Li F, Carlsson D, Doillon CJ, Nakamura M, Suuronen E, Shiozaki N, Nakata K, Sheardown H. Artificial human corneas: Scaffolds for transplantation and host regeneration. Cornea 2002; 21(Suppl 2):S54-61.

5. Eye Bank of Canada, 2007; personal communication.

6. Chirila TV. An overview of the development of artificial corneas with porous skirts and the use of PHEMA for such an application. Biomaterials 2001; 22:3311-17.

7. Marieb EN. Human Anatomy and Physiology. Menlo Park: Addison Wesley Longman Inc, 1998.

8. Rolando M, Zierhut M. The ocular surface and tear film and their dysfunction in dry eye disease. Surv Ophthalmol 2001; 45(Supp 2):S203-10.

9. Suzuki K, Saito J, Yanai R, Yamada N, Chikama T, Seki K, Nishida T. Cell-matrix and cell-cell interactions during corneal epithelial wound healing. Prog Retin Eye Res 2003; 22:113-33.

10. Lu L, Reinach PS, Kao WW. Corneal epithelial wound healing. Exp Biol Med 2001; 226:653-64.

11. Dalton BA, Evans MDM, McFarland GA, Steele JG. Modulation of corneal epithelial stratification by polymer surface topography. J Biomed Mater Res 1999; 45:384-94.

12. Fujikawa LS, Foster CS, Gipson IK, Colvin RB. Basement membrane components in healing rabbit corneal epithelial wounds: Immunofluorescence and ultrastructural studies. J Cell Biol 1984; 98:128-38.

13. Suzuki K, Tanaka T, Enoki M, Nishida T. Coordinated reassembly of the basement membrane and junctional proteins during corneal epithelial wound healing. Invest Ophthalmol Vis Sci 2000; 41:2495-500.

14. Wu XY, Cornell-Bell A, Davies TA, Simons ER, Trinkaus-Randall V. Expression of integrin and organization of F-actin in epithelial cells depends on the underlying surface. Invest Ophthalmol Vis Sci 1994; 35:878-90.

15. Wilson SE, Hong J. Bowman's layer structure and function: Critical or dispensable to corneal function? A hypothesis. Cornea 2000; 19:417-20.

16. Vaughan D. A Learning System in Histology, CD Rom and Guide. Oxford University Press, 2002. http://www.bu.edu/histology/p/08002loa.htm.

17. Hicks C, Crawford G, Chirila T, Wiffen S, Vijayasekaran S, Lou X, Fitton J, Maley M, Clayton A, Dalton P, Platten S, Ziegelaar B, Hong Y, Russo A, Constable I. Development and clinical assessment of an artificial cornea. Prog Retin Eye Res 2000; 19:149-70.

18. Welge-Lüβen U, May CA, Neubauer AS, Priglinger S. Role of tissue growth factors in aqueous humor homeostasis. Curr Opin Ophthalmol 2001; 12:94-9.

19. Streilein JW, Masli S, Takeuchi M, Kezuka T. The eye's view of antigen presentation. Hum Immunol 2002; 63:435-43.

20. Streilein JW, Stein-Streilein J. Does innate immune privilege exist? J Leukoc Biol 2000; 67:479-87.

21. George A, Pitt WG. Comparison of corneal epithelial cellular growth on synthetic cornea materials. Biomaterials 2002; 23:1369-73.

22. Chirila TV, Hicks CR, Dalton PD, Vijayasekaran S, Lou X, Hong Y, Clayton AB, Ziegelaar BW, Fitton JH, Platten S, Crawford GJ, Constable IJ. Artificial Cornea. Prog Polym Sci 1998; 23:447-73.

23. Merrett K. Interactions of corneal cells with transforming growth factor-β modified poly dimethyl siloxane surfaces. University of Ottawa 2002; MASc Thesis.

24. Hicks CR, Fitton JH, Chirila TV, Crawford GJ, Constable IJ. Keratoprostheses: Advancing toward a true artificial cornea. Surv Ophthalmol 1997; 42:175-89.

25. Duan D, Klenkler BJ, Sheardown H. Progress in the development of a corneal replacement: Keratoprostheses and tissue-engineered corneas. Expert Rev Med Devices 2006; 3:59-72.

26. Yaghouti F, Nouri M, Abad JC, Power WJ, Doane MG, Dohlman CH. Keratoprosthesis: Preoperative prognostic categories. Cornea 2001; 20:19-23.

27. Trinkaus-Randall V., Nugent MA. Biological response to a synthetic cornea. J Control Release 1998; 53:205-14.

28. Wu XY, Tsuk A, Leibowitz HM, Trinkaus-Randall V. In vivo comparison of three different porous materials intended for use in a keratoprosthesis. Br J Ophthalmol 1998; 82:569-76.

29. Legeais JM, Renard G. A second generation of artificial cornea (Biokpro II). Biomaterials 1998; 19:1517-22.

30. Dupuy FP, Salvodelli M, Robert AM, Robert L, Legeais JM, Renard G. Chemotactic penetration of keratocytes in ePTFE polymer in vitro. J Biomed Mater Res 2001; 56: 487-93.

31. Alió JL, Mulet ME, Haroun H, Merayo J, Ruiz Moreno J. Five year follow-up of biocolonisable microporous fluorocarbon haptic (BIOKOP) keratoprosthesis implantation in patients with high risk of corneal graft failure. Br J Ophthalmol 2004; 88:1585-9.

32. Kobayashi H, Ikada Y. Corneal cell adhesion and proliferation on hydrogel sheets bound with cell-adhesive proteins. Curr. Eye Res 1991; 10:899-908.

33. Capecchi JT, Franzblau C, Gibbons DF, Isaacson WB, Johnston MR, Knoll RL, Leibowitz HM, Trinkaus-Randall V. Corneal implants and manufacture and use thereof. 1992; US Patent No. 5,108,428.

34. Legeais JM, Renard G, Parel JM, Ing ETS, Salvodelli M, Pouliquen Y. Keratoprosthesis with biocolonizable microporous fluorocarbon haptic: Preliminary results in a 24-patient study. Arch Ophthalmol 1995; 113:757-63.

35. Myung D, Koh W, Bakri A, Zhang F, Marshall A, Ko J, Noolandi J, Carrasco M, Cochran JR, Frank CW, Ta CN. Design and fabrication of an artificial cornea based on a photolithographically patterned hydrogel construct. Biomed Microdevices 2007; Jan 20 [epub].

36. Myung D, Ta C, Frank CW, Koh W, Noolandi J. Interpenetrating Polymer Network Hydrogel Corneal Prosthesis. 2007; US Patent No. 20070179605.

37. Hicks CR, Crawford GJ, Lou X, Tan DT, Snibson GR, Sutton G, Downie N, Werner L, Chirila TV, Constable IJ. Corneal replacement using a synthetic hydrogel cornea, AlphaCor^{TM}: Device, preliminary outcomes and complications. Eye 2003; 17:385-92.

38. Hicks CR, Crawford GJ, Tan DT, Snibson GR, Sutton GL, Downie N, Gondhowiardjo TD, Lam DS, Werner L, Apple D, Constable IJ. AlphaCor™ Cases: Comparative outcomes. Cornea 2003; 22:583-90.

39. Stulting RD, Crawford GJ, Dart J, et al. AlphaCor artificial cornea: Clinical results to date. Abstracts, ASCRS/ASOA 2005.

40. Hicks CR, Werner L, Vijayasekaran S, Mamalis N, Apple DJ. Histology of AlphaCor skirts: Evaluation of biointegration. Cornea 2005; 24:933-40.

41. Lou X, Dalton PD, Chirila TV. Hydrophilic sponges based on 2-hydroxyethyl methacrylate. Part VII: Modulation of sponge characteristics by changes in reactivity and hydrophilicity of crosslinking agents. J Mater Sci Mater Med 2000; 11:319-25.

42. Chan GYN, Hughes TC, McLean KM, McFarland GA, Nguyen X, Wilkie JS, Johnson G. Approaches to improving the biocompatibility of porous perfluoropolyethers for ophthalmic applications. Biomaterials 2006; 27:1287-95.

43. Tjia JS, Aneskievich BJ, Moghe PV. Substrate-adsorbed collagen and cell secreted fibronectin concertedly induce cell migration on poly(lactide-glycolide) substrates. Biomaterials 1999; 2223-33.

44. Vitte J, Benoliel AM, Pierres A, Bongrand P. Is there a predictable relationship between surface physical-chemical properties and cell behaviour at the interface? Eur Cell Mater 2004; 7:52-63.

45. Roach P, Eglin D, Rohde K, Perry CC. Modern biomaterials: A review – bulk properties and implications of surface modifications. J Mater Sci: Mater Med 2007; 18:1263-77.

46. Wang Y, Robertson JL, Spillman WB, Claus RO. Effects of the chemical structure and the surface properties of polymeric biomaterials on their biocompatibility. Pharm Res 2004; 21:1362-73.

47. Evans MD, Xie RZ, Fabbri M, Madigan MC, Chaouk H, Beumer GJ, Meijs GF, Griesser HJ, Steele JG, Sweeney DF. Epithelialization of a synthetic polymer in the feline cornea: A preliminary study. Invest Ophthalmol Vis Sci 2000; 41:1674-80.

48. Latkany R, Tsuk A, Sheu MS, Loh IH, Trinkaus-Randall V. Plasma surface modification of artificial corneas for optimal epithelialization. J Biomed Mater Res 1997; 36:29-37.

49. Hsuie GH, Lee SD, Wang CC, Shiue MH, Chang PCT. ppHEMA-modified silicone rubber film towards improving rabbit corneal epithelial cell attachment and growth. Biomaterials 1993; 14:591-7.

50. Merrett K, Griffith CM, Deslandes Y, Pleizier G, Sheardown H. Adhesion of corneal epithelial cells to cell adhesion peptide modified pHEMA surfaces. J Biomater Sci Polym Ed 2001; 12:647-71.

51. Steele JG, Johnson G, McLean KM, Beumer GJ, Griesser HJ. Effect of porosity and surface hydrophilicity on migration of epithelial tissue over synthetic polymer. J Biomed Mater Res 2000; 50:475-82.

52. Diehl KA, Foley JD, Nealey PF, Murphy CJ. Nanoscale topography modulates corneal epithelial cell migration. J Biomed Mater Res 2005; 75A:603-11.

53. Karuri NW, Porri TJ, Albrecht RM, Murphy CJ, Nealey PF. Nano- and microscale holes modulate cell-substrate adhesion, cytoskeletal organization, and -β1 integrin localization in Sv40 human corneal epithelial cells. IEEE Trans Nanoscience 2006; 5:273-80.

54. Fitton JH, Dalton BA, Beumer G, Johnson G, Griesser HJ, Steele JG. Surface topography can interfere with epithelial tissue migration. J Biomed Mater Res 1998; 42:245-57.

55. Evans MDM, Taylor S, Dalton BA, Lohmann D. Polymer design for corneal epithelial tissue adhesion: Pore density. J Biomed Mater Res 2003; 64A:357-64.

56. Liliensiek SJ, Campbell S, Nealey PF, Murphy CJ. The scale of substratum topographic features modulates proliferation of corneal epithelial cells and corneal fibroblasts. J Biomed Mater Res 2006; 79A:185-92.

57. Wilson SE, Liu JJ, Mohan RR. Stromal-epithelial interactions in the cornea. Prog Retin Eye Res 1999; 18:293-309.

58. Wilson SE, Mohan RR, Mohan RR, Ambrosio R, Hong JW, Lee JS. The corneal wound healing response: Cytokine-mediated interaction of the epithelium, stroma, and inflammatory cells. Prog Retin Eye Res 2001; 20:625-37.

59. Wilson SE, Chen L, Mohan RR, Liang Q, Liu J. Expression of HGF, KGF, EGF and Receptor Messenger RNAs following corneal epithelial wounding. Exp Eye Res 1999; 68:377-97.

60. Zieske JD, Takahashi H, Hutcheon AEK, Dalbone AC. Activation of epidermal growth factor receptor during corneal epithelial migration. Invest Ophthalmol Vis Sci 2000; 41:1346-55.

61. Honma Y, Nishida K, Sotozono C, Kinoshita S. Effect of transforming growth factor-β1 and -β2 on in vitro rabbit corneal epithelial cell proliferation promoted by epidermal growth factor, keratinocyte growth factor, or hepatocyte growth factor. Exp Eye Res 1997; 65:391-6.

62. Nakamura Y, Sotozono C, Kinoshita S. The epidermal growth factor receptor (EGFR): Role in corneal wound healing and homeostasis. Exp Eye Res 2001; 72:511-7.

63. Li D, Tseng SCG. Differential regulation of keratinocyte growth factor and hepatocyte growth factor/scatter factor by different cytokines in human corneal and limbal fibroblasts. J Cell Physiol 1997; 172:361-72.

64. Wilson SE, He Y, Weng J, Zieske JD, Jester JV, Schultz GS. Effect of epidermal growth factor, hepatocyte growth factor, and keratinocyte growth factor, on proliferation, motility and differentiation of human corneal epithelial cells. Exp Eye Res 1994; 59:665-78.

65. Maldonado BA, Furcht LT. Epidermal growth factor stimulates integrin-mediated cell migration of cultured human corneal epithelial cells on fibronectin and arginine-glycine-aspartic acid peptide. Invest Ophthalmol Vis Sci 1995; 36:2120-6.

66. Ohji M, Mandarino L, SundarRaj N, Thoft RA. Corneal epithelial cell attachment with endogenous laminin and fibronectin. Invest Ophthalmol Vis Sci 1993; 34:2487-92.

67. Lim M, Goldstein MH, Tuli S, Schultz GS. Growth factor, cytokine and protease interactions during corneal wound healing. Ocular Surf 2003; 1:53-65.

68. Kitazawa T, Kinoshita S, Fujita K, Araki K, Watanabe H, Ohashi Y, Manabe R. The mechanism of accelerated corneal epithelial healing by human epidermal growth factor. Invest Ophthalmol Vis Sci 1990; 31:1773-8.

69. Imanishi J, Kamiyama K, Iguchi I, Kita M, Sotozono C, Kinoshita S. Growth factors: Importance in wound healing and maintenance of transparency of the cornea. Prog Retin Eye Res 2000; 19:113-29.

70. Fini ME. Keratocyte and fibroblast phenotypes in the repairing cornea. Prog Retin Eye Res 1999; 18:529-51.

71. Wilson SE. Stimulus-specific and cell type-specific cascades: Emerging principles relating to control of apoptosis in the eye. Exp Eye Res 1999; 69:255-66.

72. Yanai R, Yamada N, Kugimiya N, Inui M, Nishida T. Mitogenic and antiapoptotic effects of various growth factors on human corneal fibroblasts. Invest Ophthalmol Vis Sci 2002; 43:2122-6.

73. Maltseva O, Folger P, Zekaria D, Petridou S, Masur SK. Fibroblast growth factor reversal of the corneal myofibroblast phenotype. Invest Ophthalmol Vis Sci 2001; 42:2490-5.

74. Sakamoto T, Ueno H, Sonoda K, Hisatomi T, Shimizu K, Ohashi H, Inomata H. Blockade of TGF-β by in vivo gene transfer of a soluble TGF-β type II receptor in the muscle inhibits corneal opacification, edema and angiogenesis. Gene Ther 2000; 7:1915-24.

75. Sweeney DF, Xie RZ, Evans MDM, Vannas A, Tout SD, Griesser HJ, Johnson G, Steele JG . A comparison of biological coatings for the promotion of corneal epithelialization of synthetic surface in vivo. Invest Ophthalmol Vis Sci 2003; 44: 3301-9.

76. Thissen H, Johnson G, Hartley PG, Kingshott P, Griesser HJ. Two-dimensional patterning of thin coatings for the control of tissue outgrowth. Biomaterials 2006; 27:35-43.

77. Jacob JT, Rochefort JR, Bi J, Gebhardt BM. Corneal epithelial cell growth over tethered-protein/peptide surface-modified hydrogels. J Biomed Mater Res 72B; 2005:198-205.

78. Wallace C, Jacob JT, Stoltz A, Bi J, Bundy K. Corneal epithelial adhesion strength to tethered-protein/peptide modified hydrogel surfaces. J Biomed Mater Res 2005; 72A:19-24.

79. Aucoin L, Griffith CM, Pleizier G, Deslandes Y, Sheardown H. Interactions of corneal epithelial cells and surfaces modified with cell adhesion peptide combinations. J Biomater Sci Polymer Edn 2002; 13:447-62.

80. Duan X, McLaughlin C, Griffith M, Sheardown H. Biofunctionalization of collagen for improved biological response: Scaffolds for corneal tissue engineering. Biomaterials 2007; 28:78-88.

81. Jones SM, Kazlauskas A. Connecting signaling and cell cycle progression in growth factor-stimulated cells. Oncogene 2000; 19:5558-67.

82. Lauffenburger DA, Linderman JJ. (1993). Receptors: Models for Binding, Trafficking and Signaling. New York: Oxford University Press, 1993.

83. Sorkin A, von Zastrow M. Signal transduction and endocytosis: Close encounters of many kinds. Nat Rev Mol Cell Biol 2002; 3:600-14.

84. Roberts AB. The ever-increasing complexity of TGF-β signaling. Cytokine Growth Factor Rev 2002; 13:3-5.

85. Carpenter G, Cohen S. Epidermal Growth Factor. Annu Rev Biochem 1979; 48:193-216.

86. Kuhl PR, Griffith-Cima LG. Tethered epidermal growth factor as a paradigm for growth factor-induced stimulation from the solid phase. Nat. Med. 1996; 2:1022-7.

87. Ito Y. Tissue engineering by immobilized growth factors. Mater Sci Eng C 1998; 6:267-74.

88. Dinbergs ID, Brown L, Edelman ER. Cellular response to transforming growth factor-β1 and basic fibroblast growth factor depends on release kinetics and extracellular matrix interactions. J Biol Chem 1996; 271:29822-9.

89. Nathan C, Sporn M. Cytokines in context. J Cell Biol 1991; 113:981-6.

90. Jorissen RN, Walker F, Pouliot N, Garrett TPJ, Ward CW, Burgess AW. Epidermal growth factor receptor: Mechanisms of activation and signaling. Exp Cell Res 2003; 284:31-53.

91. Lee H, Park TG. Preparation and characterization of mono-PEGylated epidermal growth factor: Evaluation of in vitro biologic activity. Pharm Res 2002; 19:845-51.

92. Holladay LA, Savage CR, Cohen S, Puett D. Conformation and unfolding thermodynamics of epidermal growth factor and derivatives. Biochem 1976; 15:2624-33.

93. Taylor JM, Mitchell WM, Cohen S. Epidermal growth factor: Physical and chemical properties. J Biol Chem 1972; 5928-34.

94. Araki F, Nakamura H, Nojima N, Tsukomo K, Sakamoto S. Stability of recombinant human epidermal growth factor in various solutions. Chem Pharm Bull 1989; 37:404-6.

95. Hommel U, Harvey TS, Driscoll PC, Campbell ID. Human epidermal growth factor: High resolution solution structure and comparison with human transforming growth factor α. J Mol Biol 1992; 227:271-82.

96. Lu H, Chai J, Li M, Huang B, He C, Bi R. Crystal structure of human epidermal growth factor and its dimerization. J Biol Chem 2001; 276:34913-7.

97. Wilson SE, Schultz GS, Chegini N, Weng J, He Y. Epidermal growth factor, transforming growth factor alpha, transforming growth factor beta, acidic fibroblast growth factor, basic fibroblast growth factor, and interleukin-1 proteins in the cornea. Exp Eye Res 1994; 59:63-72.

98. Ohashi Y, Motokura M, Kinoshita Y, Mano T, Watanabe H, Kinoshita S, Manabe R, Oshiden K, Yanaihara C. Presence of epidermal growth factor in human tears. Invest Ophthalmol Vis Sci 1989; 30:1879-82.

99. Chung JH, Fagerholm P. Treatment of rabbit corneal alkali wounds with human epidermal growth factor. Cornea 1989; 8:122-8.

100. Taniguchi E, Nagae Y, Watanabe H, Ohashi Y, Kinoshita S, Manabe R. The effect of recombinant epidermal growth factor in corneal angiogenesis. Nippon Ganka Gakkai Zasshi 1991; 95:52-8.

101. Nezu E, Ohashi Y, Kinoshita S, Manabe R. Recombinant human epidermal growth factor and corneal neovascularization. Jpn J Ophthalmol 1992; 36: 401-6.

102. Hirata A, Ogawa S, Kometani T, Kuwano T, Naito S, Kuwano M, Ono M. ZD1839 (Iressa) induces antiangiogenic effects through inhibition of epidermal growth factor receptor tyrosine kinase. Cancer Res 2002; 62:2554-60.

103. Hongo M, Itoi M, Yamaguchi N, Imanishi J. Distribution of epidermal growth factor (EGF) receptors in rabbit corneal epithelial cells, keratocytes and endothelial cells, and the changes induced by transforming growth factor-β1. Exp EyeRes 1992; 54:9-16.

104. Sheardown H, Cheng YL. Mechanisms of corneal epithelial wound healing. Chem Eng Sci 1996; 51:4517-29.

105. Sheardown H, Wedge C, Chou L, Apel R, Cheng YL. Continuous epidermal growth factor delivery in corneal epithelial wound healing. Invest Ophthalmol Vis Sci 1993; 34:3593-600.

106. Grant MB, Khaw PT, Schultz GS, Adams JL, Shimizu RW. Effects of epidermal growth factor, fibroblast growth factor, and transforming growth factor-beta on corneal cell chemotaxis. Invest Ophthalmol Vis Sci 1992; 33:3292-301.

107. Nishida T, Nakamura M, Mishima H, Otori T. Differential modes of action of fibronectin and epidermal growth factor on rabbit corneal epithelial migration. J Cell Physiol 1990; 145:549-54.

108. Nakamura M, Nishida T. Potentiation by cyclic AMP of the stimulatory effect of epidermal growth factor on corneal epithelial migration. Cornea 2003; 22: 355-8.

109. Song QH, Singh RP, Trinkaus-Randall V. Injury and EGF mediate the expression of $\alpha_6\beta_4$ integrin subunits in corneal epithelium. J Cell Biochem 2001; 80:397-14.

110. Song QH, Klepeis VE, Nugent MA, Trinkaus-Randall V. TGF-β1 regulates TGF-β1 and FGF-2 mRNA expression during fibroblast wound healing. Mol Pathol 2002; 55:164-76.

111. Blake DA, Yu H, Young DL, Caldwell DR. Matrix stimulates the proliferation of human corneal endothelial cells in culture. Invest Ophthalmol Vis Sci 1997; 38:1119-29.

112. Wells A, Welsh JB, Lazar CS, Wiley S, Gill GN, Rosenfeld MG. Ligand-induced transformation by a noninternalizing epidermal growth factor receptor. Science 1990; 247:962-4.

113. Gobin AS, West JL. Effects of epidermal growth factor on fibroblast migration through biomimetic hydrogels. Biotechnol Prog 2003; 19:1781-85.

114. Bentz H, Schroeder JA, Estridge TD. Improved local delivery of TGF-β2 by binding to injectable fibrillar collagen via difunctional polyethylene glycol. J Biomed Mater Res 1998; 39:539-48.

115. Mann BK, Schmedlen RH, West JL. Tethered TGF-β increases extracellular matrix production of vascular smooth muscle cells. Biomaterials 2001; 22:439-44.

116. Ito Y, Zheng J, Imanishi Y. Enhancement of cell growth on a porous membrane co-immobilized with cell growth and cell adhesion factors. Biomaterials 1997; 18: 197-202.

117. Zisch AH, Schenk U, Schense JC, Sakiyama-Elbert SE, Hubbell JA. Covalently conjugated VEGF-fibrin matrices for endothelialization. J Contr Release 2001; 72:101-13.

118. Backer MV, Patel V, Jehning BT, Claffey KP, Backer JM. Surface immobilization of active vascular endothelial growth factor via a cysteine-containing tag. Biomaterials 2006; 27:5452-8.

119. Merrett K, Griffith CM, Deslandes Y, Pleizier G, Dubé MA, Sheardown H. Interactions of corneal cells with transforming growth factor β2-modified poly dimethyl siloxane surfaces. J Biomed Mater Res 2003; 67A:981-93.

120. DeLong SA, Moon JJ, West JL. Covalently immobilized gradients of bFGF on hydrogel scaffolds for directed cell migration. Biomaterials 2005; 26:3227-34.

121. Kapur TA, Schoichet MS. Immobilized concentration gradients of nerve growth factor guide neurite outgrowth. J Biomed Mater Res 2004; 68A:235-43.

122. Liu H, Chen C, Tsai C, Lin I, Hsiue G. Heterobifunctional poly(ethylene glycol)-tethered bone morphogenic protein-2-stimulated bone marrow mesenchymal stromal cell differentiation and osteogenesis. Tissue Eng 2007; 13:1113-24.

123. Hern DL, Hubbell JA. Incorporation of adhesion peptides into nonadhesive hydrogels useful for tissue resurfacing. J Biomed Mater Res 1998; 39:266-76.

124. Roberts MJ, Bentley MD, Harris JM. Chemistry for peptide and protein PEGylation. Adv Drug Deliv Rev 2002; 54:459-76.

125. Harris J. Poly(ethylene glycol) Chemistry: Biotechnical and Biomedical Applications. New York: Plenum, 1992.

126. Kingshott P, Thissen H, Griesser HJ. Effects of cloud-point grafting, chain length, and density of PEG layers on competitive adsorption of ocular proteins. Biomaterials 2002; 23:2043-56.

127. Veronese FM. Peptide and protein PEGylation: A review of problems and solutions. Biomaterials 2001; 22:405-17.

128. Liu L, Sheardown H. Glucose permeable poly (dimethyl siloxane) poly (N-isopropyl acrylamide) interpenetrating networks as ophthalmic biomaterials. Biomaterials 2005; 26:233-44.

129. Chen H, Chen Y, Sheardown H, Brook MA. Immobilization of heparin on a silicone surface through a heterobifunctional PEG spacer. Biomaterials 2005; 26: 7418-24.

130. Chen H, Brook MA, Sheardown HD, Chen Y, Klenkler B. Generic bioaffinity silicone surfaces. Bioconjug Chem 2006; 17:21-8.

131. Chen H, Zhang Z, Chen Y, Brook MA, Sheardown H. Protein repellant silicone surfaces by covalent immobilization of poly(ethylene oxide). Biomaterials 2005; 26:2391-9.

132. Shen G, Anand MFG, Levicky R. X-ray photoelectron spectroscopy and infrared spectroscopy study of maleimide-activated supports for immobilization of oligodeoxyribonucleotides. Nucleic Acids Res 2004; 32:5973-80.

2.0 METHODS

2.1 Surface Preparation

2.1.1 Plasma Polymerization

Plasma polymerization is a commonly used technique for introducing reactive functional groups on the surface of a material without affecting the bulk properties. Cold gas plasmas may be generated by radio or microwave frequency excitation of a gas at low pressure, with microwave frequencies often leading to a higher density of active species [1]. Plasmas contain a range of species including ions, neutrals, radicals, electrons, excited species and photons [2]. Under optimal conditions, the plasma components are believed to polymerize and attach chemically to the underlying substrate, resulting in a thin, highly-crosslinked and defect-free film [3]. A further advantage is the applicability to a wide range of device geometries for use *in vitro* and *in vivo* [4]. Plasma polymerization of allylamine was used in this work to produce a surface with reactive amine functionalities for subsequent conjugation of PEG. While the mechanism of allylamine polymerization is not fully understood, and both ions and oligomers play a role in the mass deposition [2], several models including the one in Figure 2-1 below have been proposed. The high energy of the plasma may affect other bond sites besides the C=C bond, and the associated rearrangement of monomer atoms may lead to functional groups including secondary or tertiary amines and imines not expected to be observed

under conventional polymerization [2,5]. Subsequent surface relaxation of the plasma-modified materials over time may also occur, as has been demonstrated for PDMS [6,7].

Microwave frequency plasma polymerization was performed in this work using a custom-built plasma reactor [3]. Allylamine monomer was degassed, and the reactor was evacuated to a pressure below 50 μm Hg. Surfaces were exposed first to argon plasma at a flow rate of 235 scm for 5 minutes, followed by allylamine monomer at a flowrate of 0.9 scm for 10 minutes. The forward power was maintained at 20W and the reflected power was less than 2W during the run; the reactor pressure during allylamine excitation was approximately 90 μm Hg. Following the reaction, the allylamine flow was stopped. Once the pressure had re-stabilized, the reactor was backfilled with argon and the samples removed. Surfaces were rinsed in Milli-Q water and dried overnight under vacuum.

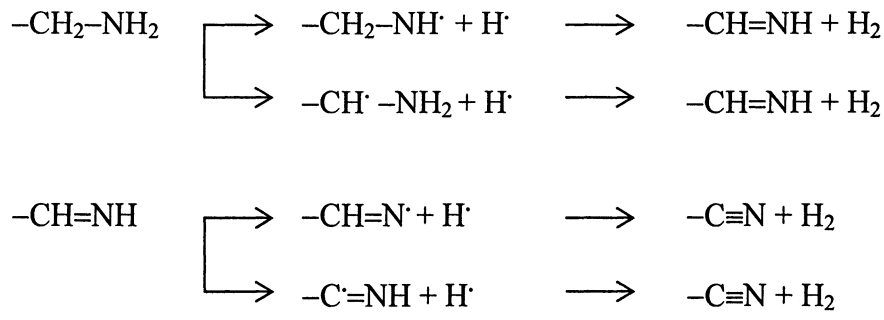

Figure 2-1. Proposed mechanisms of allylamine plasma polymerization [adapted from 5].

2.2 Analysis and Optimization of EGF-PEG Reaction

2.2.1 SDS PAGE and Western Blotting

Sodium dodecyl sulfate polyacrylamide gel electrophoresis (SDS-PAGE) is a method of separating molecules according to size [8]. Proteins are first mixed with SDS in order to remove secondary structure and apply a uniform mass-to-charge ratio, and with a reducing agent (e.g. β-mercaptoethanol) to break disulfide bonds. This allows the distance of migration through the gel to be directly related to only the size of the protein. The denatured proteins are subsequently injected into one end of a polyacrylamide gel, and an electric current is applied across the gel. Proteins will then migrate preferentially based on their size and associated resistance in traveling through the pores of the gel. Upon completion of the run, the protein bands in the gel are electrophoretically transferred to a polyvinylidene fluoride membrane. At this point, colloidal gold staining of the membrane may be used to observe the protein bands. Western blotting may also be performed to identify specific proteins within the bands. In this procedure, the membrane is incubated with a primary antibody to the protein of interest, and alkaline phosphatase conjugated secondary antibody directed against the primary antibody is then applied. Reaction of the alkaline phosphatase with a chromogenic substrate indicates the presence of the various proteins on the membrane.

SDS-PAGE and Western blotting were used in this work in order to identify relative amounts of EGF pegylation reaction products, which were expected to have higher molecular weights than unreacted EGF. Samples were prepared by reacting EGF

(50 μg/mL) with PEG at a range of molar ratios, reaction times and pH values, after which the reaction was quenched by addition of glycine to a concentration of 25 mM. A detailed procedure for the gel electrophoresis and blotting may be found in Appendix A.1.

2.2.2 MALDI Mass Spectrometry

Matrix-assisted laser desorption ionization mass spectrometry (MALDI) is a technique for measuring the molecular weight and purity of an analyte with a very high mass resolution and low detection limit. The analyte is mixed with an excess of an organic matrix, typically a small organic acid, to form a bed of co-crystallized analyte-matrix mix. The sample is then irradiated by a pulsed laser beam under high vacuum, from which the matrix absorbs most of the energy leaving the analyte intact. Volatilization of the matrix leads to formation of a dense gas cloud and transfer of energy from matrix to analyte. Collisions between the analyte and excited matrix ions results in protonation or deprotonation of analyte molecules. Through the use of a time-of-flight (TOF) analyzer, these ions are separated by their velocity from which the mass to charge ratio can be determined [9]. While MALDI is highly sensitive for detection of small proteins, the mass resolving power decreases as molecular weight increases [10], and the low pH of the matrix may potentially impact the structure of the analyte. It is also noted that the technique only semi-quantitative and as such requires parallel experiments for quantification [11].

MALDI was used in this work to verify the molecular weights of the EGF-PEG reaction products. EGF was diluted in water to 50 μg/mL and reacted with PEG at a 1:50

molar ratio for 20 minutes, at which point the reaction was quenched by addition of glycine to a concentration of 25 mM and the samples were transferred to a -70°C freezer until further use. Measurements were made with a Micromass (Manchester) TofSpec 2E spectrometer with a nitrogen laser at 337 nm. Samples were run in linear mode using sinapinic acid as a matrix.

2.3 Material Surface Characterization

2.3.1 Water Contact Angles

Sessile drop water contact angle measurement is a straightforward technique for determining the interfacial free energy of a surface. A drop of liquid, typically water, is placed on the material, and the contact angle between the fluid and water determined visually as shown in Figure 2-2a [12]. Contact angles, which are sensitive to the outer 3 to 10 Å of the surface, are a convenient method for rapidly assessing changes in hydrophobicity or hydrophilicity of a surface upon modification [13]. Additionally, differences between this angle upon increase and decrease of the drop volume, termed advancing and receding contact angles, provide a measure of surface roughness and/or heterogeneity [14]. It is noted, however, that contact angle data may be significantly affected by factors including impurities on the surface or in the test fluid, surface topography and heterogeneity, droplet size, and time to acquire readings, and as such it is mainly limited to assessing relative changes between surfaces. Additionally, reorientation of the surface structure upon exposure to the test fluid must be considered [12]. For

assessing hydrated surfaces, underwater contact angle measurement with air as the test fluid is performed using the captive bubble technique (Figure 2-2b).

In this work, sessile drop and captive bubble contact angles on control and modified PDMS surfaces were obtained using a Ramé-Hart NRL 100-00 goniometer (Mountain Lakes, NJ). A drop volume of 10 μL was used for all measurements.

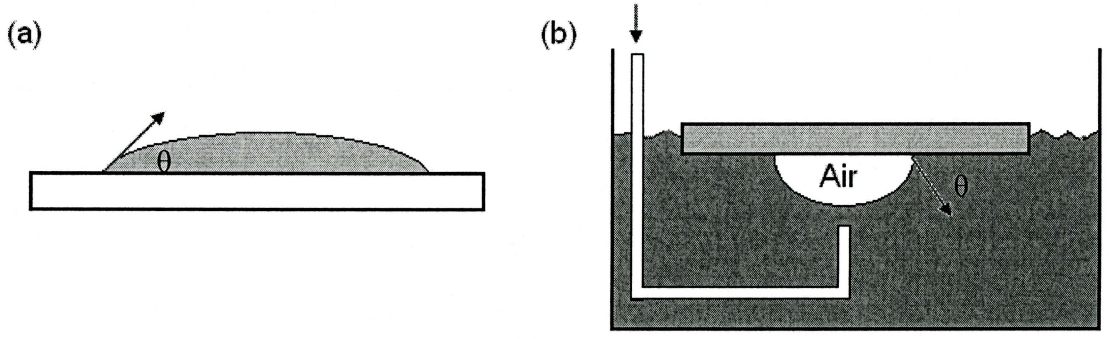

Figure 2-2. Contact angle measurement by a) sessile drop and b) captive bubble methods [adapted from 12].

2.3.2 X-Ray Photoelectron Spectroscopy

X-ray photoelectron spectroscopy (XPS), or elemental spectroscopy for chemical analysis (ESCA), is a technique frequently used to determine the elemental composition of a material surface. Upon irradiation of the sample under ultra-high vacuum by a beam of monochromatic x-rays, photoelectrons are emitted which have kinetic energies specific to the elements present as well as to their chemical state (Figure 2-3) [15]. The intensity of the emitted signal provides a quantitative measure of the species abundance. As the emitted electrons have limited ability to penetrate through the material beyond a maximum depth of 100 Å, the analysis is surface-specific, and all elements except

hydrogen or helium can be detected to a sensitivity of approximately 0.1 atom percent [16,17]. Typically, low resolution (1000 eV wide) survey scans are first performed to identify the different elements present, then high resolution (20 eV wide) scans are used to acquire more detailed information about chemical shifts of specific elements from which the associated chemical bond environment may be inferred. Additionally, by variation of the takeoff angle at which the samples are irradiated (termed "angle-resolved" XPS), compositional variation as a function of sampling depth can be analyzed. It is noted that XPS results are sensitive to the presence of impurities at the material surface, and may also be affected by rearrangement of surface molecules under the high vacuum conditions [12].

In this work, XPS analysis was performed at Surface Interface Ontario using a Leybold MAX 200 XPS System (Cologne, Germany), using a non-monochromatised Mg K_α X-ray source operating at 15 kV and 20 mA. The spot size used was 2x4 mm. The energy range was calibrated by placing the Au 4f peak at 84 eV or the main C1s peak at 284.5 eV. Survey scans were performed from 0 to 1000 eV, and low resolution and high resolution C1s spectra were obtained at 90^o and 20^o takeoff angles. Specslab software (Specs, Berlin) was used for data fitting.

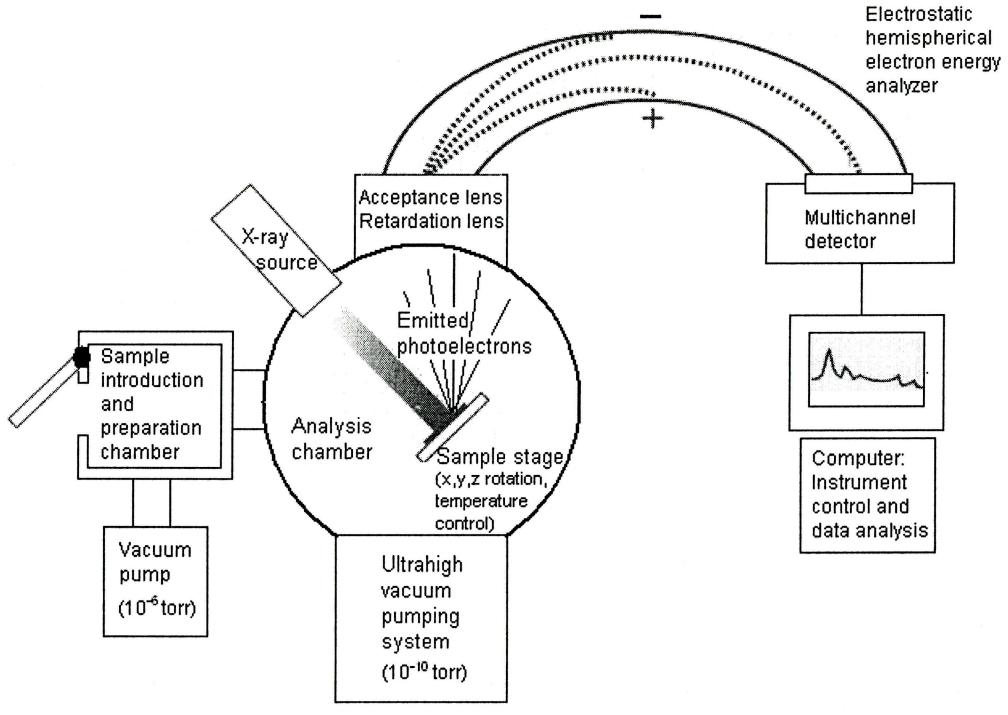

Figure 2-3. Schematic of x-ray photoelectron spectroscopy (XPS) analysis [adapted from 12].

2.3.3 Attenuated Total Reflection Fourier Transform Infrared Spectroscopy (ATR-FTIR)

Attenuated Total Reflection Fourier Transform Infrared Spectroscopy (ATR-FTIR) is a means of analyzing molecular structure on a surface, by measuring the frequency of IR radiation required to excite vibrations in molecular bonds [18]. In ATR mode, an interface is established between the sample and an internal reflection element (crystal) with a different index of refraction. The electromagnetic waves are entirely reflected back into the internal reflection element in order to increase the intensity of the surface versus the bulk signal [Figure 2-4] [19]. While IR is typically employed as a bulk characterization method, use of ATR instrumentation results in a sample penetration depth ranging from 1 to 5 μm [12].

ATR-FTIR spectroscopy was carried out using a BioRad FTS-40 spectrometer (Cambridge MA) with Harrick ATR apparatus and thallium bromide-chloride crystal. 32 scans were performed for each sample. Background signals from atmospheric carbon dioxide and water were be removed by purging of the apparatus with nitrogen.

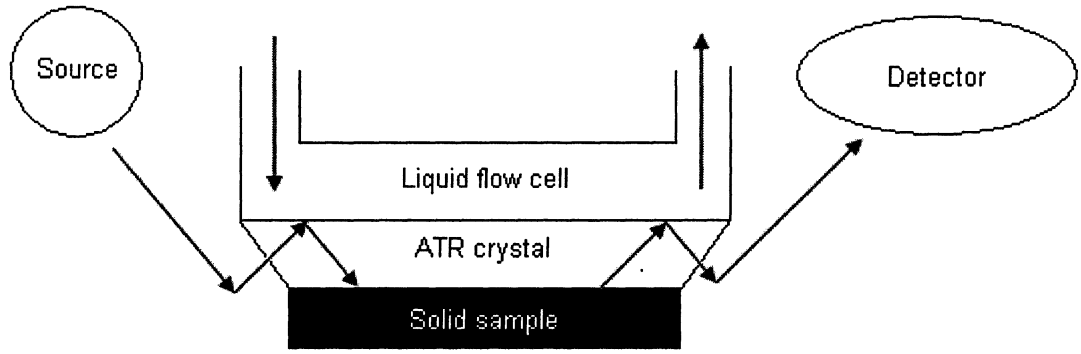

Figure 2-4. Sample analysis by attenuated total reflection Fourier transform infrared spectroscopy (ATR-FTIR) [adapted from 12].

2.3.4 Radioiodonation

Radioiodonation is a radiolabelling procedure frequently used for the quantification of bound proteins on a biomaterial surface. In this process, radioactive iodine is introduced into tyrosine residues on the protein of interest [20].

In this work, radioiodonation of EGF was performed using the Iodogen method (Pierce, Rockford, IL). Reaction vials were obtained precoated with Iodogen reagent, 1,3,4,6-tetrachloro-3a,6a-diphenyl-glycoluril, which oxidizes the iodine enabling electrophilic attack on the ortho position of the aromatic ring on the tyrosine [21]. 200 μg of EGF was dissolved in PBS (1 mg/mL) and added to an Iodogen vial with 5 uL of ^{125}I, and the reaction was allowed to proceed for 15 minutes. To remove unreacted ^{125}I, the

reaction solution was injected into a MW 3400 dialysis cassette, and overnight dialysis was performed against cold PBS with three changes of buffer. The free iodide percentage following dialysis was determined using trichloroacetic acid (TCA) precipitation as shown in Appendix A.2, and was in the range of 5 to 8%. The concentration of labeled EGF was determined spectrophotometrically using an extinction coefficient of 3.025 [ε (1%, 280 nm)] as provided by the supplier. The labeled EGF was then diluted to the appropriate concentrations and tethered to the modified PDMS surfaces, and the surface radioactivity measured with a gamma counter. For experiments on gold-coated wafers, PBS-NaI buffer was used instead of PBS to inhibit the adsorption of free ^{125}I to the surfaces as has been shown previously [22]. Solution counts of known EGF concentrations were used to convert surface radioactivity into bound protein amounts.

2.3.5 Surface Plasmon Resonance

Surface Plasmon Resonance (SPR) is an optical technique which has recently gained usage in analysis of protein interactions with polymeric materials [23,24]. The principle of SPR operation is shown in Figure 2-5. A monochromatic light source is shone through a gold-coated glass sensor chip and is totally internally reflected at the gold interface, with an evanescent wave penetrating into the less dense medium on the opposite side of the gold film. At a critical angle of incident light, the evanescent wave couples with free oscillating electrons (plasmons) in the gold film, leading to resonant excitation of the plasmons and a corresponding decrease in intensity of reflected light. The critical angle for SPR is dependent on the refractive index of the medium above the

gold surface (to a distance of 300 nm) [23,24]. Hence binding of proteins to the material on the gold surface, leading to a change in mass and therefore refractive index, will lead to a shift in the SPR angle (expressed as Resonance Units (RU), or 10^{-5} degrees of an angle) which can be monitored throughout a binding experiment. Previous studies have shown the SPR signal to increase linearly with mass of bound protein [25]. SPR allows detection of binding to picogram quantities of biomolecules, without the need for labeling [25]. Additionally, because experiments are done under flow, binding kinetics can be monitored in situ [23]. Limitations include the requirement to coat a thin layer of the polymer under study on a gold substrate, with layer thicknesses below 100 nm optimal for SPR signal detection.

SPR experiments were performed using a Biacore 2000 instrument (Biacore, Piscataway, NJ). Polymer-modified gold chips were first exposed to degassed phosphate buffered saline (PBS) at a flow rate of 25 μL/min until a stable baseline was reached. A high flowrate was chosen to minimize mass transfer effects on binding. This was followed by injection of the protein solution, and subsequent reintroduction of buffer to remove loosely adsorbed material. Differences in Resonance Units before and after injection were calculated.

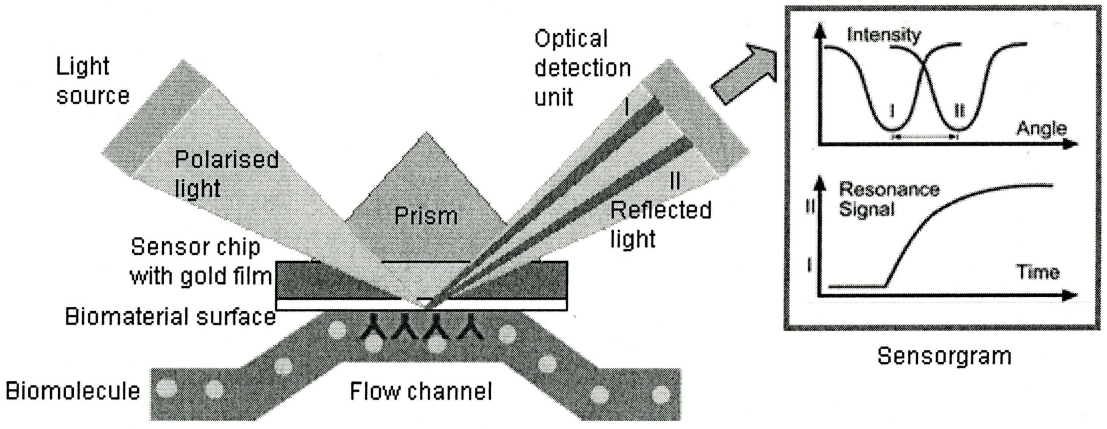

Figure 2-5. Surface plasmon resonance (SPR) operation [adapted from 26].

2.3.6 Surface Profilometry

White light optical profiling employs the technique of interferometry for analysis of surface topography [27]. White light is shone through a beam splitter, which directs the light to both the sample surface and to a reference mirror as shown in Figure 2-6. Upon recombination of the two beams of reflected light, a pattern of interference "fringes" forms, with maximum fringe contrast occurring at the best focus position for each point on the sample. Either the test sample or the measurement head is scanned vertically such that each point on the surface passes through focus. Mapping of the height of each point on the surface allows for sub-nanometer resolution to be attained. Surface profilometry measurement provides a rapid method for analysis of biomaterials compared with atomic force microscopy (AFM), and has been shown to yield similar values of surface roughness [28].

Surface profilometry studies were conducted with a Veeco WYKO NT1100 optical profiler (Woodbury, NY) equipped with Vision32 software to image the surface texture.

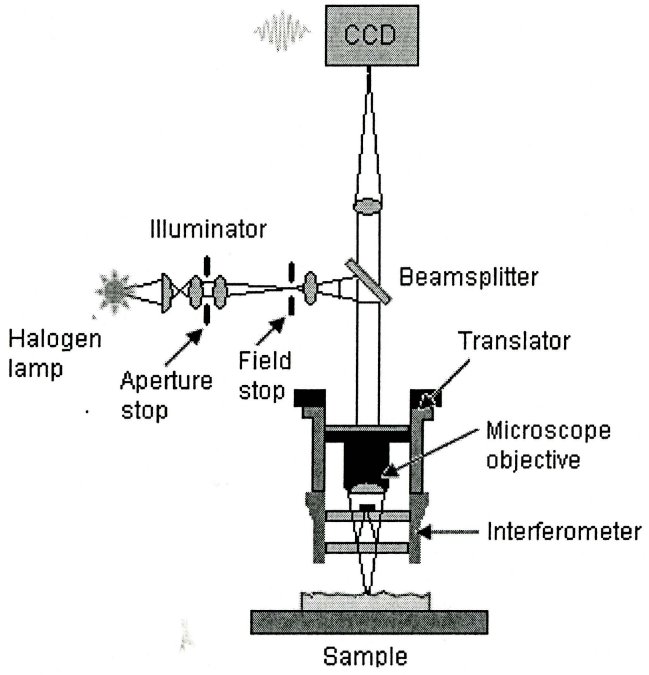

Figure 2-6. Schematic of white light interferometry technique used for optical profiling [adapted from 29].

2.3.7 Ellman's Reagent Assay

Ellman's Reagent, 5,5'-dithiobis-(2-nitrobenzoic acid), or DTNB, is used for colourimetric assay of thiol functional groups. Upon reaction of this water-soluble reagent with accessible thiols, it forms a mixed disulfide and liberates the chromophore 5-mercapto-2-nitrobenzoic acid in solution with absorption maximum at 410 nm [30,31].

Ellman's Reagent was used in this work for determination of surface thiol density on modified PDMS substrates. A 140 μM solution of Ellman's Reagent in PBS was

prepared. Surfaces were placed in a 96-well plate and 250 μL of Ellman's Reagent solution was added and incubated for 30 minutes. Standard solutions were made up of known concentrations of 3-mercaptopropyltrimethoxysilane in isopropyl alcohol, and 50 μL of each standard was added to 250 μL of Ellman's Reagent solution in the 96-well plate for 30 minutes. PDMS samples were then removed from the wells and the absorbance of the solutions read at 415 nm using a plate reader. Readings from unmodified PDMS discs were used as controls.

2.4 Biological Surface Characterization

2.4.1 Corneal Epithelial Cell Culture

The biological activity of the EGF-modified surfaces was examined through measurement of human corneal epithelial cell culture growth *in vitro*. High passage immortalized human corneal epithelial cells (HCEC) were previously screened for morphological, biochemical, and electrophysiological similarities to cells obtained from postmortem human corneas [32]. A detailed procedure for seeding of the cells on the surfaces is found in Appendix A.3. Unless specifically noted, Keratinocyte Serum Free Medium used for growth experiments was prepared without the addition of exogenous EGF or bovine pituitary extract, to isolate the specific effects of the surface-bound EGF on cell growth. At specific time points during the culture period, surfaces were analyzed by inverted light microscopy using a 10x or 20x objective. For quantification of cell growth, cells were detached from surfaces by trypsinization and counted. Culture medium

was removed from each well, and 250 μL of trypsin added to cover each surface. After 10 minutes of incubation, 250 μL of Dulbecco's Modified Eagle's Medium (DMEM) containing 10% fetal bovine serum was added to each well, and the medium thoroughly mixed by pipetting to dislodge remaining cells. The cell suspension was transferred to eppendorf tubes. An additional 500 μL of DMEM was used to rinse each well which was added to the cell suspensions in the eppendorf tubes. The samples were then counted immediately using a Beckman Coulter counter with a 1:7 ratio of suspension to Isoton II diluent.

2.4.2 Immunostaining

Immunostaining experiments were performed to analyze the expression of extracellular matrix proteins and associated integrin receptors by the cells on the modified substrates. A detailed procedure is located in Appendix A.4. Fixed and stained surfaces were observed using fluorescence microscopy at 20x magnification.

Confocal microscopy was also used to examine the localization of integrin receptors within the cell layers on the surfaces. In confocal microscopy, point illumination and a pinhole in an optically conjugate plane in front of the detector function to eliminate out-of-focus light and glare from the sample. As only the light within the focal plane can be detected, a superior image is provided versus conventional wide-field microscopy, and image resolutions of 0.2 and 0.6 μm in the x-y and z planes, respectively, can be achieved [33]. By scanning points across the focal plane of the sample, two-dimensional pictures can be generated and compiled to form three-

dimensional images. A Zeiss LSM 510 laser scanning microscope at 63x magnification and slice thickness of 1 μm was used in this work.

2.4.3 Cell Adhesion Assay

The adhesion of corneal epithelial cells to surfaces under an applied detachment force is critical for an artificial cornea application. The simplest and most common adhesion assay involves washing off non-adherent cells and subsequent counting of remaining cells. However such assays are limited by a lack of sensitivity and reproducibility. Other quantitative assays based on micromanipulation and hydrodynamic shear require specialized equipment and/or time- and skill-sensitive operation. Centrifugation assays, in contrast, have been shown to provide a simple and robust means for assessing cell adhesion to a variety of biomaterial surfaces [34].

In this work, cell adhesion was assessed according to the method of Reyes and Garcia by measuring calcein-AM fluorescence, a membrane-permeable indicator of cell viability, before and after application of a centrifugal force [34]. Cells on the surfaces were incubated in medium containing 5 μM of calcein-AM. This medium was then removed, and surfaces were fastened using double-sided tape to the bottom of new wells of a 48-well plate which were then filled with PBS. The fluorescence at 485/518 nm excitation/emission was read using a Thermo Fluoroskan Ascent fluorimeter. Plates were then covered with sealing film, and centrifuged upside down at 900 rpm (189g) for 5 minutes. The PBS in the wells was replaced with fresh PBS and the fluorescence was remeasured.

2.4.4 Reverse Transcription Polymerase Chain Reaction (RT-PCR)

Reverse Transcription Polymerase Chain Reaction (RT-PCR) is a powerful tool for amplification and quantification of ribonucleic acid (RNA) sequences in order to assess levels of cellular gene expression. Single-stranded RNA extracted from the cells is used to make complementary DNA (cDNA) through the process of reverse transcription. DNA primers bind to the 3' end of the RNA, and initiate assembly of deoxyribonucleotides (dNTPs) in a complementary sequence to the RNA template by reverse transcriptase, an RNA-dependent DNA polymerase enzyme. In the next step, polymerase chain reaction (PCR) is performed to amplify the DNA. Primers to the DNA segment of interest hybridize with their complementary sequence, and along with a temperature-resistant DNA polymerase enzyme, initiate assembly of dNTPs into double-stranded DNA. Heating of the reaction products over 95°C melts the two DNA strands apart, and subsequent lowering of the temperature again enables another round of synthesis to begin. Repeated raising and lowering of the temperature rapidly amplifies the sequence of interest [8].

Real-time quantification of gene sequences of interest may be achieved using several fluorescence techniques. One method is based on the use of TaqMan probes, oligonucleotides with a fluorescent reporter dye attached to the 5' end and a quencher moeity coupled to the 3' end. These probes specifically hybridize to an internal sequence of a PCR product. During PCR, replication by DNA polymerase of the strand on which a TaqMan probe is bound causes cleavage of the probe. This in turn decouples the fluorescent dye and the quencher, so that quenching no longer occurs and fluorescence is

detected. The level of fluorescence is proportional to the amount of polymerization and probe cleavage [35].

In this work, preliminary experiments were performed to assess levels of EGF and EGF receptor (EGFR) expression by cells growing on the modified surfaces. After 5 days of culture, cells were trypsinized from modified and control surfaces as described above, pooled from 3 samples for each surface type and centrifuged at 300g for 5 minutes. The cell pellets were then subjected to RNA isolation and purification using a Qiagen RNeasy Mini Kit (Qiagen N.V., Netherlands) according to the manufacturer's instructions. The RNase free DNase set (Qiagen) was used in conjunction with the kit for DNase digestion during the RNA purification step. The RNA concentration within the resulting samples was determined spectrophotometrically to range from 28 to 110 μg/mL. Integrity of the RNA was tested using an Agilent RNA 6000 Pico Assay kit and Agilent 2100 Bioanalyzer (Agilent Technologies Inc, Santa Clara, CA). Only samples with clear marker and ribosomal peaks and an RNA integrity number over 6.8 were used in the remainder of the process.

Two rounds of RNA amplification were performed using an Ambion Message II aRNA Amplification Kit (Ambion Inc, Austin TX), according to the manufacturer's instructions. Following amplification, the RNA concentrations in the samples were 2058 to 3405 μg/mL. 5 μg of each sample was then used for cDNA synthesis; a detailed procedure for this step is located in Appendix A.5. TaqMan gene expression assays were obtained from Applied Biosystems (Foster City, CA) containing target-specific primers for human EGF (assay HS00153181_m1) and EGFR (assay HS00193306_m1). The PCR

amplification protocol from this supplier was followed using an ABI Prism 7700 Sequence Detection System. Samples were measured in triplicate, and GAPDH was used as a housekeeping gene for normalization of gene expression levels.

2.5 References

1. Sodhi RNS, Sahi VP, Mittelman MW. Application of electron spectroscopy and surface modification techniques in the development of anti-microbial coatings for medical devices. J Elec Spect Rel Phenom 2001; 121:249-64.

2. Beck AJ, Candan S, Short RD, Goodyear A, Braithwaite NSJ. The role of ions in the plasma polymerization of allylamine. J Phys Chem B 2001; 105:5730-6.

3. Wickson BM, Brash JL. Surface hydroxylation of polyethylene by plasma polymerization of allyl alcohol and subsequent silylation. Coll Surf A: Physicochem Eng Aspects 1999; 156:201-13.

4. Kingshott P, Thissen H, Griesser HJ. Effects of cloud-point grafting, chain length, and density of PEG layers on competitive adsorption of ocular proteins. Biomaterials 2002; 23:2043-56.

5. Krishnamurthy V, Kamei IL, Wei Y. Analysis of plasma polymerization of allylamine by FTIR. J Polym Sci Part A: Polym Chem 1989; 27:1211-24.

6. Chen IJ, Lindner E. The stability of radio-frequency plasma-treated polydimethylsiloxane surfaces. Langmuir 2007; 23:3118-22.

7. Williams RL, Wilson DJ, Rhodes NP. Stability of plasma-treated silicone rubber and its influence on the interfacial aspects of blood compatibility. Biomaterials 2004; 25:4659-73.

8. Lodish H, Baltimore D, Berk A, Zipursky SL, Matsudaira P, Darnell J. Molecular Cell Biology (3rd Edn.) New York: Scientific American Books, Inc., 1999.

9. Kicman AT, Parkin MC, Isles RK. An introduction to mass spectrometry based proteomics - Detection and characterization of gonadotropins and related molecules. Mol Cell Endocrinol 2007; 260-262:212-27.

10. Gross ML. Mass spectrometry in the biological sciences: A tutorial. Series C: Mathematical and Physical Sciences. Boston: Kluwer Academic Publishers, 1992.

11. McLean KM, McArthur RC, Chatelier RC, Kingshott P, Griesser HJ. Hybrid biomaterials: Surface-MALDI mass spectrometry analysis of covalent binding versus physisorption of proteins. Coll Surf B: Biointerfaces 2000; 17:23-35.

12. Ratner BD, Hoffman AS, Schoen FJ, Lemons JE. Biomaterials Science (2nd Edn.) San Diego: Elsevier Academic Press, 2004. pp. 40-59.

13. Johnston EE, Ratner BD. Surface characterization of plasma deposited organic thin films. J Electron Spectroscopy Related Phenom, 1996; 81:303-17.

14. Chibowski E. Surface free energy of a solid from contact angle hysteresis. Adv Coll Interface Sci 2003; 103:149-72.

15. Werner C, Jacobasch HJ, Reichelt G. Surface characterization of hemodialysis membranes based on streaming potential measurements. J Biomater Sci Polym Ed 1995; 7:61-76.

16. Ratner BD, Tyler BJ, Chilkoti A. Analysis of biomedical polymer surfaces: polyurethanes and plasma-deposited thin films. Clin Mater 1993; 13:71-84.

17. Jablonski A. Quantitative surface analysis by X-ray photoelectron spectroscopy. Polish J Chem 2000; 11:1533-66.

18. Ratner BD, Chilkoti A, Castner DG. Contemporary methods for characterizing complex biomaterial surfaces. Clin Mater 1992; 11:25-36.

19. Barbucci R, Casolaro M, Magnani A. Characterization of biomaterial surfaces: ATR-FTIR, potentiometric and calorimetric analysis. Clin Mater 1992; 11:37-51.

20. Regoezci E. Iodine labeled plasma proteins, Boca Raton: CRC Press, 1984.

21. Salacinski, PR, McLean C, Sykes JE, Clement-Jones VV, Lowry PJ. Iodination of proteins, glycoproteins, and peptides using a solid-phase oxidizing agent, 1,3,4,6-tetrachloro-3a,6a-diphenyl-glycoluril (Iodogen). Anal Biochem 1981; 117:136-46.

22. Du YJ, Cornelius RM, Brash JL. Measurement of protein adsorption to gold surface by radioiodination methods: Suppression of free iodide sorption. Coll Surf B: Biointerfaces 2000; 17:59-67.

23. Green RJ, Frazier RA, Shakesheff KM, Davies MC, Roberts CJ, Tendler SJB. Surface plasmon resonance analysis of dynamic biological interactions with biomaterials. Biomaterials 2000; 21:1823-35.

24. Davies J. Surface plasmon resonance: The technique and its applications to biomaterial processes. Nanobiol 1994, 3:5-16.

25. Stenberg E, Persson B, Roos H, Urbaniczky C. Quantitative determination of surface concentration of protein with surface plasmon resonance using radiolabeled proteins. J Coll Interface Sci 1991; 143:513-26.

26. www.biacore.com

27. Hariharan P. Interferometers. In: Handbook of Optics. New York: McGraw-Hill Companies, Inc., 1996.

28. Bourauel C, Fries T, Drescher D, Plietsch R. Surface roughness of orthodontic wires via atomic force microscopy, laser specular reflectance, and profilometry. Eur J Orthod 1998; 20:79-92.

29. www.veeco.com

30. Hu ML. Measurement of protein thiol groups and glutathione in plasma. Methods Enzymol 1994; 233:380-5.

31. Jocelyn PC. Spectrophotometric assay of thiols. Methods Enzymol 1987; 143: 44-67.

32. Griffith M, Osborne R, Munger R, Xiong X, Doillon CJ, Laycock NL, Hakim M, Song Y, Watsky MA. Functional human corneal equivalents constructed from cell lines. Science 1999; 286:2169-72.

33. Shotton DM. Electronic light microscopy: Present capabilities and future prospects. Histochem Cell Biol 1995; 104:97-137.

34. Reyes CD, Garcia AJ. A centrifugation cell adhesion assay for high-throughput screening of biomaterial surfaces. J Biomed Mater Res 2003; 67A:328-33.

35. www.ambion.com

3.0 CONTRIBUTIONS TO ARTICLES

The following describes my contributions to the articles comprising Chapters 4 through 9. I was responsible for the literature searches, experimental design and data analysis for all of the papers. The majority of the experimental work was carried out by myself, with several exceptions. For Paper 1, MALDI experiments were conducted by Dr. Kirk Green in the Department of Chemistry at McMaster University. For Paper 2, the initial cell culture experiment was conducted by Cecilia Becceril in the laboratory of May Griffith at the University of Ottawa, prior to establishment of culture facilities in our own laboratories. All subsequent cell culture experiments were carried out by myself using this protocol and cell lines supplied by the Griffith lab. X-ray photoelectron spectroscopy (XPS) data was obtained with the assistance of Dr. Rana Sodhi at the University of Toronto. For Paper 3, development of immunostaining procedures on the surfaces was carried out with the assistance of Dr. Dhruva Dwivedi, in the laboratory of Dr. Judy West-Mays in the Department of Pathology and Molecular Medicine at McMaster. For Papers 4 and 5, the generic surface modification techniques were initially developed in the McMaster Department of Chemistry by Dr. Hong Chen, Dr. Yang Chen, Lihua Liu and Jill Ranger in the laboratory of Dr. Michael Brook. I adapted these techniques for the tethering of EGF specific to my project. For Papers 5 and 6, surface profilometry experiments were performed, and additional repeat samples for XPS were prepared, by Renita D'souza in the McMaster Department of Chemistry. For Paper 6, I modified a surface modification strategy initially developed by Dr. Amro Ragheb and Dr. Yang

Chen in the McMaster Department of Chemistry in the laboratory of Dr. Michael Brook. I developed and optimized an alternate application for this technique in order bind surface thiol groups for the subsequent tethering of pegylated EGF. I generated the first draft of all the papers, and worked with my supervisor on subsequent drafts and on addressing comments from reviewers.

In addition to the papers included within this thesis, my experimental data are also contained within the following paper authored by Dr. Hong Chen:

Chen H, Brook MA, Sheardown HD, Chen Y, Klenkler B. Generic bioaffinity silicone surfaces. Bioconjug Chem 2006; 17:21-8.

I am also the primary author for the following two review articles:

Klenkler B, Sheardown H. Growth factors in the anterior segment: role in tissue maintenance, wound healing and ocular pathology. Exp Eye Res 2004; 79:677-88.

Klenkler B, Sheardown H, Jones L. Growth factors in the tear film: role in tissue maintenance, wound healing, and ocular pathology. Ocul Surf 2007; 5:228-39.

Additionally I am a co-author for the following review article:

Duan D, Klenkler BJ, Sheardown H. Progress in the development of a corneal replacement: keratoprostheses and tissue-engineered corneas. Expert Rev Med Devices 2006; 3:59-72.

10.0 SUMMARY AND FUTURE WORK

In this thesis, three different methods for the attachment of EGF to PDMS substrates via PEG chains were developed and examined for their effect on corneal epithelial cell growth. The differing results from the three methods provide insights into the effects of surface-bound EGF and the importance of the underlying tethering chemistry for artificial cornea and other applications.

The first method (Plasma Modification) employed a "solution-first" scheme in which EGF was first bound to homobifunctional NHS_2PEG in solution, then exposed to allylamine plasma-modified PDMS substrates. Use of SDS-PAGE for optimization of the EGF-PEG prereaction indicated that a 1:50 ratio of EGF to PEG provided the highest reaction yield. Subsequent surface binding led to EGF densities in the range of 40 to 90 ng/cm^2 as measured by ^{125}I radiolabelling and SPR, however a maximum of approximately 30% of this was covalently tethered even under optimal prereaction conditions. This is likely due to competing hydrolysis reactions inherent with this homobifunctional chemistry, formation of multipegylated species as detected by SDS-PAGE, faster adsorption versus covalent binding reactions, and the relatively undefined nature of the underlying allylamine plasma polymer layer. Additional optimization, for example by molecular weight separation of mono- and multi-pegylated species, is precluded by relatively rapid hydrolysis of the free NHS group on the homobifunctional PEG compared with the length of time required to perform the separation.

Despite the heterogeneity of the surface EGF binding, *in vitro* cell culture experiments indicated that the bound EGF was indeed active in promoting growth of corneal epithelial cells on the modified substrates over this concentration range. Cell numbers, adhesion under detachment force and extracellular matrix protein production were all significantly increased on EGF-modified versus control substrates, indicating that the modification presents a promising strategy for promotion of epithelialization on these substrates. PDMS surfaces with EGF adsorbed directly also showed high levels of cell growth, however coverage was less uniform and adhesion to the surfaces was significantly lower than on those with pegylated EGF.

Several additional studies are required to further develop these surfaces for use in an artificial cornea application. The cellular response over longer time periods (weeks to months), and in fluid with similar composition to human tears, must be analyzed. The ability of the cells to form and renew stratified multilayers similarly to those in the native cornea must also be determined. Physiologically relevant studies of the effect of shear force on cell adhesion, for example using a flow apparatus, should be undertaken. The effect of the bound EGF on promoting cell migration, such as from the surrounding limbal tissue, must be addressed, for example in organ culture experiments. A gradient of tethered EGF may be further beneficial in guiding cell growth over the materials. These studies will assist in dictating the eventual means of applying these surfaces in an artificial cornea; the surfaces may either be implanted directly and stimulate migration of epithelial cells from the remaining host tissue and subsequent adhesion and proliferation, or the surfaces may be preseeded with cells prior to implantation for which the bound

EGF stimulates their rapid initial coverage. Simultaneous binding of other growth factors, such as NGF for reestablishment of corneal innervation and promotion of epithelial cell survival [1], through these methods presents further opportunities for improvements to current models. Additionally, because PDMS alone is not amenable to diffusion of nutrients for cell survival, the EGF surface modification must eventually be applied to PDMS that is bulk-modified, for example with interpenetrating poly-NIPAAm networks to enhance glucose permeability [2]. As the EGF binding technique described is not substrate specific, this approach is expected to be feasible. Finally, as relatively high levels of cell coverage were also observed visually on surfaces where EGF was entrapped within the PEG layer on the surface (versus covalently bound), it would be of interest to more conclusively compare results from the tethered growth factor surfaces to those that provide controlled release of EGF, to determine the optimal presentation strategy for an artificial cornea application *in vivo*.

While promising initial biological results were observed on the Plasma Modified EGF-tethered surfaces, the inherent binding heterogeneity prevents the elucidation of the specific effects of covalently tethered versus adsorbed EGF. As has been hypothesized and demonstrated in a small number of previous studies, tethered biomolecules are expected to retain increased activity versus those that are adsorbed directly. As such, a conformationally homogenous surface is desired to more readily predict and control the associated biological response. To address this concern, a second "surface-first" tethering scheme (Method 2, Hydrosilylation) was used to produce EGF-tethered substrates. In this method, PDMS was first modified with SiH groups to bind heterobifunctional allyl-PEG-

NHS. Two variations of this approach were used: the "direct" method (where allyl-PEG-NHS was bound directly to PDMS), and the simpler, more stable "indirect" method (where allyl-PEG-OH was bound and subsequently converted to PEG-NHS). Upon exposure to solutions of EGF of various concentrations, different amounts of EGF were bound via the free NHS group on the PEG. Bound EGF concentrations on the order of 10 to 300 ng/cm^2 were attained by both Hydrosilylation methods, of which between 80 and 90% was covalently bound, representing a significant improvement over the Plasma Modified surfaces.

However, the results of cell culture experiments on the Hydrosilylation surfaces were less promising than those synthesized by Plasma Modification. With both the direct and indirect methods, cell growth was increased by the presence of EGF, but was slower than on the Plasma Modified surfaces at the same time points and confluence was not reached across the entire surfaces. Surfaces produced by the direct method showed a slow but EGF concentration-dependent increase in cell numbers, while PEG-only modified control surfaces completely inhibited the growth of cells on the PDMS. The higher density of the PEG tethering layer on these surfaces (versus Plasma Modification), which is required to prevent adsorption of free EGF to the PDMS and is confirmed by XPS and protein radiolabelling studies, appears to be inhibitory to protein deposition and cell adhesion and spreading across the surfaces. This is in contrast to the allylamine substrate layer used in the Plasma Modification scheme, which does not hinder and may possibly stimulate cell adhesion. A maximal level of cell stimulation by EGF was not reached, despite the high concentrations of the surface-bound growth factor. On surfaces produced

by the indirect Hydrosilylation method, no concentration effect of the EGF was observed, and inhibition of cell growth by PEG was less pronounced and only noted at lower seeding densities. This may be an effect of surface topography, which indicates that the PEG may be bound in clusters and could potentially hinder spreading of cells across the surfaces in a uniform manner and mask concentration effects of the bound EGF. Surprisingly, simultaneous binding of the cell adhesion peptide YIGSR had no further stimulatory effect on cell growth, indicating that a maximal level of spreading and adhesion had been reached with the EGF modification alone. Together the results indicate that the Hydrosilylation technique for tethering EGF is not optimal for use in an artificial cornea application.

Further analysis may be carried out to determine the reasons for the lack of confluent cell coverage on the Hydrosilylation surfaces particularly at high EGF surface concentrations. The distribution of EGF binding across the surfaces may be investigated through the use of immunostaining and phase AFM imaging. The positive cell coverage results from surfaces previously generated using this method for binding of the cell adhesion peptide RGD [3,4] indicate that specifically EGF binding and/or signaling to its receptor is hindered or altered by the tethering methodology used. It is possible that use of a higher molecular weight PEG chain may more readily allow for receptor binding, mobility within the cell membrane and dimerization required for growth factor signaling. Methods to readily bind longer PEG chains by hydrosilylation, while preserving a PEG surface conformation that inhibits free protein adsorption, will require development. Other possible strategies to overcome the inhibitory effect of the underlying tethering

layer include the concurrent binding of alternate cell adhesion molecules (e.g. RGD), use of alternate tethering polymers, or release of the EGF either via a labile tether structure or directly from the polymer layer.

Based on the results from the first two methods, a third EGF tethering scheme, Thiol Modification, was developed to combine the optimal features from the previous methods. In this procedure, EGF was first reacted in solution with a heterobifunctional NHS-PEG-maleimide. PDMS substrates modified with 3-mercaptopropyltrimethoxy silane were then exposed to the EGF-PEG solution, upon which tethering occurs by the rapid and selective thiol-maleimide reaction. The increased stability of the maleimide group enables the EGF-PEG reaction to be carried out for longer time periods than with the Plasma Modification method, further reducing the amount of unbound EGF that can be adsorbed to the PDMS surfaces. Additionally, due to the solution-first approach used, a lower PEG density on the surfaces is required compared with the Hydrosilylation method, and can be controlled by varying the PEG concentration in solution. EGF surface concentrations ranging from 24 to 65 ng/cm^2 were bound using the conditions studied; as hypothesized, a much larger fraction of EGF remained bound after SDS rinsing than on the Plasma Modified surfaces (78% vs 30%), indicating more homogeneous covalent binding. Due to the demonstrated stability of the maleimide end group, further improvements may possibly be achieved in future by molecular weight separation of mono- and multipegylated EGF prior to exposure to the thiolated surfaces.

Surprisingly, cell culture experiments indicated that the presence of thiol groups inhibited the spreading and growth of corneal epithelial cells on the PDMS substrates,

even in the presence of bound EGF. Similarly, lens epithelial cell coverage was also inhibited even in serum-containing conditions, suggesting that this observation was not specific to corneal epithelial cells. Normal cell morphology and growth could be restored on the PDMS by reacting surface thiol groups with 3-maleimidopropionic acid, indicating that such capping reactions are required to retain the proliferative effect of the bound growth factor. A further alternative may be the adsorption of adhesion proteins or peptides between the PEG chains on the PDMS substrates.

The mechanism of inhibition of cell growth by the thiolated surfaces is a subject of interest for future work. To verify that the inhibition is due specifically to thiols and not the general hydrophobic nature of the silane-modified surface, experiments with other silane-containing surface modifiers of differing polarities, and various silane densities, should be conducted. Differences in conformation and denaturation of extracellular matrix and serum proteins on the thiol-modified versus the similarly hydrophobic unmodified PDMS substrates may be examined, for example by antibody binding or use of fluorescently labeled proteins [5,6]. A further mechanistic possibility, the alteration of dynamic thiol-disulfide oxidoreduction within the cell membrane and associated integrin-mediated adhesion and/or EGF receptor activity, may be investigated; probing changes in the oxidoreductive state of membrane-bound proteins would provide additional insight into this potential mechanism [7]. Finally, the surface modification method developed in this work may be extended to additional applications where epithelial and other cell coverage of a device is unwanted.

A notable observation in this thesis is that despite tethering of EGF in overlapping surface density ranges, the cellular response to the surfaces prepared by the three modification methods was markedly different. Because the EGF pegylation reaction was based on the NHS chemistry for all three methods, it is expected that the orientation of the tethered EGF on the surfaces should be comparable. It therefore appears that the underlying tethering chemistry used to bind the EGF has a highly significant effect on corneal epithelial cell coverage of the surfaces, more so than the EGF surface concentration. This is unlike the demonstrated effects of EGF in solution, where a maximal biological response is known to exist due to downregulation of the associated cellular receptors.

The mechanistic reasons for these differences would be of interest for further investigation, as the knowledge would aid in the design of EGF- and other growth factor-tethered polymeric substrates. The extent of EGF receptor binding, activation and signaling on the different surface types could be measured and compared. Approaches may include receptor binding studies on the EGF-modified surfaces, and immunostaining of cells growing on the surfaces using antibodies for the cytoplasmic terminus of the activated, phosphorylated receptor. To address the apparent lack of role of EGF concentration, EGF receptor expression levels of cells on the different surfaces could be monitored by RT-PCR. Preliminary results of EGF receptor expression on Plasma Modified and control surfaces determined by this technique are contained in Appendix B. Initial observations indicate that some differences in expression level, inversely related to the amount of EGF on the surfaces, are present. It is possible that on surfaces modified

with EGF (non-tethered) only, internalization of receptor-ligand complexes may occur leading to the similar cell proliferation results as on EGF-tethered surfaces. Further repeat experiments, experiments with other bound EGF concentrations, and with surfaces prepared by the other modification methods are required to validate these observations.

There are numerous additional directions for further improvements to the EGF-modified surfaces described in this work and to tethering of growth factors in general. Methods such as atom transfer radical polymerization (ATRP), or click chemistry, may be investigated for the synthesis of functionalized polymeric tethers with a range of defined molecular weights, for more direct examination of the effect of the tether in the different surface modification methods. The controlled spacing of the bound ligands, or formation of bridged complexes of two EGF molecules, may be attempted (for example using branched PEG chains) in order to promote EGF receptor dimerization required for activation. Tethering of EGF via a free cysteine group introduced into the protein would potentially result in further improved binding homogeneity and biological activity versus the less specific NHS-amine binding methodology [8]. Finally, the use of defined micro- and nanoscale topographical features [9,10] and regions of EGF binding on the PDMS surfaces may more specifically direct cellular responses and mimic the natural corneal epithelial tissue *in vivo*.

10.1 References

1. You L, Kruse FE, Völcker HE. Neurotrophic factors in the human cornea. Invest Ophthalmol Vis Sci 2000; 41:692-702.

2. Liu L, Sheardown H. Glucose permeable poly (dimethyl siloxane) poly (N-isopropyl acrylamide) interpenetrating networks as ophthalmic biomaterials. Biomaterials 2005; 26:233-44.

3. Chen H, Brook MA, Sheardown HD, Chen Y, Klenkler B. Generic bioaffinity silicone surfaces. Bioconjug Chem 2006; 17:21-8.

4. Mikhail AS. Peptide-modified PDMS: Surface modification for improved vascular cell interactions. McMaster University 2006; MASc Thesis.

5. Baugh L, Vogel, V. Structural changes of fibronectin adsorbed to model surfaces probed by fluorescence resonance energy transfer. J Biomed Mater Res 2004; 69A:525-34.

6. Iuliano DJ, Saavedra SS, Truskey GA. Effect of the conformation and orientation of adsorbed fibronectin on endothelial cell spreading and the strength of adhesion. J Biomed Mater Res 1993; 27:1103-13.

7. Laragione T, Bonetto V, Casoni F, Massignan T, Bianchi G, Gianazza E, Ghezzi P. Redox regulation of surface protein thiols: Identification of integrin α-4 as a molecular target by using redox proteomics. Proc Nat Acad Sci USA 2003; 100:14737-41.

8. Backer MV, Patel V, Jehning BT, Claffey KP, Backer JM. Surface immobilization of active vascular endothelial growth factor via a cysteine-containing tag. Biomaterials 2006; 27:5452-8.

9. Yim EK, Reano RM, Pang SW, Yee AF, Chen CS, Leong KW. Nanopattern-induced changes in morphology and motility of smooth muscle cells. Biomaterials 2005; 26:5405-13.

10. Kidambi S, Udpa N, Schroeder SA, Findlan R, Lee I, Chan C. Cell adhesion on polyelectrolyte multilayer coated polydimethylsiloxane surfaces with varying topographies. Tissue Eng 2007; 13:2105-17.

APPENDIX A: EXPERIMENTAL PROCEDURES

A.1: SDS-PAGE and Western Blotting Procedure

1. Polyacrylamide Gel Preparation (15% separating gel, 4% stacking gel)

Acrylamide/Bis (30% stock solution):

	Acrylamide/Bis	29.2 g
	N,N'-Methylenebisacrylamide	0.8 g

Dissolve reagents in 100 mL of Milli-Q water and filter.

15% Separating Gel:	Milli-Q water	2.4 mL
	1.5M Tris-HCl, pH 8.8	2.5 mL
	10% (w/v) SDS stock (room temp)	100 µL
	Acrylamide/Bis (30% stock)	5.0 mL

Degas above 4 reagents for 15 minutes at room temperature.

Add:	10 % ammonium persulfate (fresh)	50 µL
	TEMED	5 µL

Clean casting plates and insert into casting assembly. Fill gel plates with polymer solution, leaving enough space to add stacking gel later. Layer a small amount of water over gel. Allow the separating gel to polymerize for 1 hour before adding stacking gel.

4% Stacking Gel:	Milli-Q water	3 mL
	0.5M Tris-HCl, pH 6.8	1.2 mL
	10% (w/v) SDS stock (room temp)	100 µL
	Acrylamide/Bis (30% stock)	0.65 mL

Degas above 4 reagents for 10 minutes at room temperature.

Add:	10 % ammonium persulfate (fresh)	25 µL
	TEMED	5 µL

Fill remainder of gel plates with stacking (4%) polymer solution. Add comb for 10-well gels. Allow to polymerize for 1 hour before use.

2. Sample Preparation

Prepare samples by adding the appropriate amount to the Sample Buffer (SDS reducing buffer).

Sample Buffer (also referred to as tracking dye, TD):

Milli-Q water	4 mL
0.5M Tris HCl, pH 6.8	1.0 mL
Glycerol	0.8 mL

10 % (w/v) SDS	1.6 mL

Mix the above 4 reagents, aliquot into 225 µL volumes and store at 4°C until used.

Immediately prior to use, add: (to 225 uL aliquot)

2-Bmercaptoethanol	30 µL
0.05% (w/v) Bromophenol blue	30 µL

Samples for a 10-well gel are prepared as follows:

(Lane 1) 1 µL SDS-PAGE MW standards (broad range), 10 µL TD
(Lanes 2-9) 20 µL protein sample, 10 µL TD
(Lane 10) 7.5 µL SDS-PAGE prestained markers (broad range)

The above samples are placed in 95°C water for 7.5 minutes.

3. Electrophoresis

Electrophoresis Buffer: (5X stock solution, pH 8.3)
This buffer is made ahead of time and stored at 4°C for up to 1 month.

Tris Base	15 g
Glycine	72 g
SDS	5 g

Fill to 1 L with water. Check pH. Do not adjust with NaOH or HCl. Just before use dilute to 1X strength.

Remove combs from gels and rinse wells with Milli-Q water. Remove gels from casting stand, and place into clamp assembly. Place clamp assembly into buffer chamber. Fill upper buffer chamber to 3 mm below outer long glass plate with electrophoresis buffer. Fill lower buffer chamber until 1 cm of gel is covered with electrophoresis buffer. Add samples onto gels. Operate power pack at 200 volts for approximately 45-50 minutes of electrophoresis. Layer a small quantity of Pyronin Y dye (in sample buffer) into wells just before the tracking dye (TD) reaches the bottom of the separating gel. Continue the electrophoresis until the dye has just reached the top of the separating gel.

4. Gel Equilibration

Transfer Buffer: 3.03 g Tris
14.4 g glycine
200 mL methanol

Fill to 1 L with water. pH should be ~8.3. Do not adjust with NaOH or HCl.

Remove gels and place in cold transfer buffer for 15-20 minutes.

5. Electrophoretic Transfer

Use Immobilon PVDF transfer membrane cut to size of the gels. Prewet membranes with 100% methanol (1-3 seconds), water (1-2 minutes) and soak in transfer buffer. Load gels and membranes in transfer cassette according to manufacturers' specifications and place in transfer chamber. Fill chamber with cold transfer buffer so that the entire gel surface is covered. Blot for 1 hour at 100 V.

The membranes can then be immediately stained with colloidal gold (Step 6), or air dried for subsequent Western blotting (Step 7).

6. Gold Staining

Phosphate buffered saline (PBS), pH 7.4:

Na_2HPO_4	1.32 g
NaH_2PO_4-H_2O	0.342 g
NaCl	8.5 g

Mix reagents in Milli-Q water, adjust pH to 7.4 and dilute to 1 L.

If PVDF membrane has air dried, dip membrane in methanol, then water. Block unbound membrane sites by incubating membrane in phosphate buffered saline (PBS) containing 0.3% Tween 20 for 1 hour. Wash 3 times (1 minute each) with Milli-Q water.

Stain 1 to 4 hours, or overnight in Protogold solution (BioCell Research Laboratories, Cardiff, UK). Rinse membrane extensively with water. Air dry.

7. Western Blotting

Molecular weight determination: Remove marker lane and small portion of sample lane. Block for 1 hr in Tween-PBS. Rinse with Milli-Q water, 3 times. Stain using Protogold as described above.

Block unbound membrane sites: Wet remainder of membrane with 100% methanol, and rinse with Milli-Q water. Incubate for 1h, with gentle agitation, in 5% w/v nonfat dry milk in TBS, pH 7.4. This procedure blocks the areas of the membrane devoid of bound proteins so that nonspecific binding of antibodies to these areas will not occur. Wash 3 times for 5 minutes in 0.1% (w/v) nonfat dry milk in TBS.

Incubate with primary antibody: Incubate for 1h in 1% (w/v) nonfat dry milk, 0.05% (v/v) Tween 20 in TBS containing the first antibody to the protein of interest. Use an antibody dilution according to the supplier's specification.

Wash away unreacted material: Wash membrane as before, in 0.1% (w/v) nonfat dry milk in TBS.

Incubate with second antibody: Incubate membrane for 1h in 1% (w/v) nonfat dry milk, 0.05% (v/v) Tween 20 in TBS containing alkaline phosphatase-conjugated second antibody at 1/1000 dilution.

Wash away excess and nonspecific probe: Wash the membrane as before, in 0.1% (w/v) nonfat dry milk in TBS

Detect: Incubate with the substrate, 5-bromo-4-chloro-3-indolyl phosphate (BCIP), and nitroblue tetrazolium (NBT), to develop the colour reaction. Stop reaction by rinsing with Milli-Q water.

The following is a list of pertinent solutions:

TBS

50 mM Tris
150 mM NaCl
Adjust pH to 7.4

Carbonate Buffer

20 mg MgCl2 6H20
840 mg NaHCO3
Fill to 100 mL with Milli-Q water, and pH with NaOH to 9.8

NBT & BCIP

Dissolve 30 mg NBT in 300 μL H20, 700 μL DMF
Dissolve 15 mg BCIP in 1000 μL DMF
Add above reagents to 100 mL of carbonate buffer just before use.
Note: these reagents are light sensitive with a maximum working time of 1 hour.

A.2: Determination of Free Iodide Concentration by Trichloroacetic Acid (TCA) Precipitation of the Protein

1. Into two vials (A, B), add 990 μL of phosphate buffered saline (PBS) and 10 μL of the iodinated protein solution.
2. Into two other vials, add 990 μL of a 1% (w/v in Milli-Q water) bovine serum albumin (BSA) solution, 10 μL of the iodinated protein solution, and 500 μL of a 20% TCA solution. Vortex, wait for 10 minutes, then spin in a microcentrifuge for 0.5 minutes.
3. Into each of four vials (C-F), add 500 μL of the supernatant of the centrifuged vials and 500 μL of PBS.
4. Count all vials in the gamma counter for 1 minute.
5. Calculate the free iodide content as follows:

$$\%\ Free\ Iodide = 300 \times \left(\frac{Average\,(Vials\,C-F)}{Average\,(Vials\,A,B)} \right)$$

A.3: Human Corneal Epithelial Cell Culture and Seeding of Surfaces

Cell Thawing

Keratinocyte Serum Free Medium (Gibco #17005-042) should be prepared by adding the following supplements to the bottle:

- Penicillin/streptomycin (Gibco #15140-122): 1:100 dilution
- Gentamycin (Gibco #15710-064): 1:1000 dilution
- Epidermal growth factor (add contents of vial)
- Bovine pituitary extract (add contents of vial)

1. Prepare a 10 cm petri dish by adding 10 mL of KSFM 10 mL and let equilibrate for 30 minutes.
2. Remove cryovial from storage.
3. Holding the cryovial, dip the bottom ¾ of the cryovial in a 37°C water bath and swirl gently for 1-2 minutes until the last sliver of ice melts.
4. Remove the cryovial immediately, wipe it dry and rinse with 70% ethanol.

Cell Seeding

After cells are thawed:

1. Remove the cap, being careful not to touch the interior threads.

2. Using a micropipette with a 1000 mL tip set to 800 mL, put the tip into the cryovial and resuspend the cells.
3. Dispense the cells into the petri dish.
4. Replace the cover of the dish and gently rock to evenly distribute the cells.
5. Place the dish into a 37°C, 5% CO_2 incubator. Lay the dish flat on the shelf.
6. Change the growth medium the next day after the seeding. Let fresh medium warm up to room temperature. Use a pipette-aid to remove the medium and dispense fresh medium into the dish (approximately 10 mL for a 10 cm dish).
7. Examine cells daily using a microscope. When cells appear healthy, growth medium should be changed every 2-3 days. Note: if cells are allowed to become overconfluent and stay at confluence for more than 2 days, they can suffer irreversible contact inhibition.

Note: If there are not many cells in the dish after seeding, thaw two or three vials. Transfer the contents to a centrifuge tube, and spin at 1500 rpm for 5 minutes in a clinical centrifuge. Remove the supernatant with a pipette, then resuspend the pellet in 5 mL of KSFM, and transfer to a 6 cm dish.

Cell Splitting

Once cells are confluent in the dish:

1. Allow 1x trypsin-EDTA and fetal bovine serum (FBS) to thaw and warm to room temperature.
2. Remove KSFM and Dulbecco's Modified Eagle Medium (DMEM) from fridge and allow to warm to room temperature.
3. Remove medium from culture dish using a pipette-aid.
4. Rinse cells with 1 to 2 mL of KSFM and remove the KSFM from the dish.
5. Add trypsin (1 mL for a 10 cm dish) to the dish, and rock the dish gently to ensure cells come in contact with the trypsin.
6. Incubate the cells at 37°C for 5 to 10 minutes until the cells detach.
7. After cells are detached, add a few mL of DMEM containing 10% FBS to the dish to neutralize the trypsin. Pipette the medium up and down several times to rinse and collect the majority of the cells. Collect the medium in a 15 or 50 mL conical tube and repeat several times.
8. Spin the tube at 900 rpm (200 g) for 5 minutes in a clinical centrifuge to pellet the cells.
9. Carefully remove the supernatant, and resuspend the pellet in a small volume of KSFM.
10. The cells can then be divided for seeding into several dishes containing KSFM, as described in the Cell Seeding instructions.

Cell Freezing

1. Perform steps 1 to 8 in the Cell Splitting instructions.
2. Carefully remove the supernatant, and resuspend the pellet in 1 mL of DMEM containing 10% FBS and 10% DMSO.
3. Transfer the suspension to a cryovial.
4. Freeze cryovial in -80 °C freezer at least overnight, then transfer frozen cryovial into liquid nitrogen for storage.

Culturing of Sample Surfaces

1. Incubate surfaces in KSFM supplemented with penicillin/streptomycin and gentamycin for 24 hours.
2. Rinse surfaces two times with KSFM supplemented with penicillin/streptomycin and gentamycin.
3. Perform steps 1 to 9 in the Cell Splitting instructions
4. Mix cells well to ensure a uniform suspension, then count the cells in a small amount of suspension volume (e.g. 5 mL) using a hemocytometer.
5. Dilute the cells to the appropriate density for seeding. For ¼" polymer discs, typical seeding density is $1x10^4$ cells in 40 µL of medium (250 cells per µL).
6. Transfer surfaces to a 48-well tissue culture plate and let them dry slightly. To ensure surfaces stay submerged, medical grade silicone tubing (sterilized in ethanol) may be placed around the edges of the surfaces.
7. Add cells as a small droplet (e.g. 40 µL) to the top of the surfaces, and let the cells adhere for 15 to 20 minutes in the incubator.
8. Carefully add 250 µL of medium and return the plate to the incubator.
9. Change the medium every 2-3 days. Carefully remove 150 µL and replace with fresh medium down the sides of the well. Ensure the surfaces remain submerged.

A.4: Immunostaining Procedure

Fixing Cells

After the desired time period of culture, fix the cells on the surface as follows:
1. Make a solution of 50% acetone and 50% methanol. Put in -20°C freezer until cold.
2. Remove cell culture medium from wells containing the surfaces.
3. Add acetone/methanol solution (ensure surfaces are submerged). Leave for 2 minutes.
4. Remove acetone/methanol and let surfaces air dry.
5. Add sterile PBS to the wells. Surfaces can be kept at 4 °C for staining at a later time.

Staining Cells

1. Remove PBS from wells.

2. Add 500 μL of Triton-X (0.2% v/v in PBS) solution per well to permeabilize the cells. Leave for 5 minutes.
3. Remove PBS-Triton. Add 200 μL per well of Normal Goat Serum (NGS) solution (25 μL NGS in 500 μL of sterile PBS) to block the surfaces. Leave for 20 minutes.
4. Remove the NGS and add 200 μL per well of primary antibody solution. This should be made up according to the recommended dilution by the supplier. Leave for one hour. Keep at least one sample as a negative control (leave in NGS – do not incubate in primary Ab).
5. Remove primary Ab. Wash 2 x 5 minutes in 500 μL PBS-Triton per surface.
6. Remove PBS-Triton. Add the appropriate secondary antibody. The secondary Ab solution should be made up as follows: for 150 μL solution, mix 2.25 μL of NGS, 3 μL of secondary Ab, and 144.75 μL sterile PBS. Add 150 or 200 μL of secondary Ab solution to each well (ensure surfaces are covered). Leave for one hour in the dark.
7. Remove secondary Ab. Wash 3 x 5 minutes in 500 μL Triton-PBS in the dark.

Mounting Surfaces

1. Remove PBS-Triton. Place surfaces (cell-side up) on a clean glass slide.
2. Put a small drop of PBS-Triton on the slide to wet it. Ensure there are no air bubbles.
3. Put a drop of Vectashield mounting medium for fluorescence on the surfaces, and one drop on the slide.
4. Carefully place a coverslip over the surface. Ensure there are no air bubbles.
5. Slides can then be stored in the fridge (protected from light). If desired, the edges of the coverslip can be sealed the next day.
6. The slides are now ready for fluorescence microscopy.

A.5: Synthesis of cDNA for RT-PCR

1. Mix and briefly centrifuge each component before use.

2. Prepare the RNA/Primer mixture in sterile 0.5 mL tubes as follows:

Total 2-5 μg total RNA, diluted with RNase free water	11 μL
Random hexamers (50 ng/μL)	1 μL
10 mM dNTP mix	1 μL

3. Incubate each sample at 65°C for 5 mins and incubate on ice for at least 1 min.

4. Prepare the following reaction mixture adding each component in the indicated order:

5X 1st Strand	4 μL
0.1 M DTT	2 μL
RNaseOUT Recombinant	1 μL

5. Add 7 μL of reaction mixture to each RNA/Primer mixture, mix gently, and collect by brief centrifugation.

6. Incubate at 25°C for 2 minutes.

7. Add 1 μL (50 units) of SUPERSCRIPT II RT to each tube, mix, and incubate at 25°C for 10 minutes.

8. Heat the samples as follows:
   42°C for 50 minutes
   70°C for 15 minutes
   Add 1 μL RNase H, mix gently
   37°C for 20 minutes

9. Store the cDNA samples at -20°C or continue with Real Time Quantitative PCR.